

RESEARCH ARTICLE

Modelling the mitigation of anti-vaccine opinion propagation to suppress epidemic spread: A computational approach

Sarah Alahmadi^{1*}, Rebecca Hoyle², Michael Head³, Markus Brede¹

1 School of Electronics and Computer Science, University of Southampton, Southampton, United Kingdom, **2** School of Mathematical Sciences, University of Southampton, Southampton, United Kingdom, **3** Clinical Informatics Research Unit, Faculty of Medicine, University of Southampton, Southampton, United Kingdom

* sha1a21@soton.ac.uk



Abstract

Information regarding vaccines from sources such as health services, media, and social networks can significantly shape vaccination decisions. In particular, the dissemination of negative information can contribute to vaccine hesitancy, thereby exacerbating infectious disease outbreaks. This study investigates strategies to mitigate anti-vaccine social contagion through effective counter-campaigns that disseminate positive vaccine information and encourage vaccine uptake, aiming to reduce the size of epidemics. In a coupled agent-based model that consists of opinion and disease diffusion processes, we explore and compare different heuristics to design positive campaigns based on the network structure and local presence of negative vaccine attitudes. We examine two campaigning regimes: a static regime with a fixed set of targets, and a dynamic regime in which targets can be updated over time. We demonstrate that strategic targeting and engagement with the dynamics of anti-vaccine influence diffusion in the network can effectively mitigate the spread of anti-vaccine sentiment, thereby reducing the epidemic size. However, the effectiveness of the campaigns differs across different targeting strategies and is impacted by a range of factors. We find that the primary advantage of static campaigns lies in their capacity to act as an obstacle, preventing the clustering of emerging anti-vaccine communities, thereby resulting in smaller and unconnected anti-vaccine groups. On the other hand, dynamic campaigns reach a broader segment of the population and adapt to the evolution of anti-vaccine diffusion, not only protecting susceptible agents from negative influence but also fostering positive propagation within negative regions.

OPEN ACCESS

Citation: Alahmadi S, Hoyle R, Head M, Brede M. (2025) Modelling the mitigation of anti-vaccine opinion propagation to suppress epidemic spread: A computational approach. PLoS ONE 20(3): e0318544. <https://doi.org/10.1371/journal.pone.0318544>

Editor: Hocine Cherifi, Université de Bourgogne: Université de Bourgogne, FRANCE

Received: June 7, 2024

Accepted: January 18, 2025

Published: March 20, 2025

Copyright: © 2025 Alahmadi et al. This is an open access article distributed under the terms of the [Creative Commons Attribution License](https://creativecommons.org/licenses/by/4.0/), which permits unrestricted use, distribution, and reproduction in any medium, provided the original author and source are credited.

Data availability statement: All relevant data are within the manuscript and its [Supporting information](#) files.

Funding: SA acknowledges support from the Government of Saudi Arabia and Taibah University for her scholarship. The funders had no role in study design, data collection and analysis, decision to publish, or preparation of the manuscript.

Competing interests: The authors have declared that no competing interests exist.

Introduction

Throughout history, diseases have posed a constant threat to human health and wellbeing, with the COVID-19 pandemic serving as a recent and striking example. Vaccination is a vital tool for combating disease prevalence. However, in many instances, the availability of vaccinations does not necessarily lead to their uptake owing to several factors, including vaccine

hesitancy. According to the WHO, vaccination hesitancy is one of the top ten threats to public health [1]. One significant factor contributing to it is exposure to vaccine misinformation [2]. Furthermore, this behaviour can spread socially through imitation [3], resulting in negative collective behavior towards vaccination. This highlights the social dilemma inherent in vaccination, a topic that has been extensively studied in the literature (e.g., [4–7]). Therefore, achieving high vaccine uptake to suppress vaccine-preventable diseases remains a significant challenge for public health administration. The existing literature on coupled models of disease and behavioral diffusion is extensive, addressing different perspectives. For example, one set of studies focuses on the dynamics of awareness/misinformation/opinion-disease interactions (e.g., [8–13]). Another set addresses the problem as a vaccination game using game-theoretic frameworks (e.g., [3–5, 14, 15]). Other studies explore a combination of these approaches (e.g., [16–18]).

Information about a disease and attitudes around vaccination play a significant role in people's willingness to get vaccinated and, therefore, the extent and severity of an outbreak [19]. COVID-19 is the most recent example of the influence of misinformation on epidemic dynamics [20, 21]. Studying misinformation and vaccine opinion diffusion not only helps in understanding the range of influences on people's attitudes, but also helps in understanding the flow of attitudes across the social network and, therefore, allows for more effective intervention control strategies. Many studies have investigated the role of information dissemination on the scale of transmission of an epidemic. This information may positively serve as a trigger for self-protection, for example when awareness of a disease spreads, as in [9, 10, 12, 21], where the authors investigate how the spread of awareness may reduce the size of an epidemic. On the other hand, it may work as a stimulant for negative behavioural responses, such as the spread of false information regarding vaccinations over a social network, which negatively influences people's inclination to vaccinate [8, 11, 13, 18, 22–25].

Opinions regarding vaccines spread among individuals as a social contagion and significantly affect the distribution of vaccination coverage, subsequently influencing the transmission dynamics of diseases. Previous studies have explored the interplay between disease spread and the propagation of vaccine-related opinions. Some studies have focused on dynamics of anti-vaccine opinions while neglecting the influence of pro-vaccine propagation [11, 24, 25]. Others have examined both anti-vaccine and pro-vaccine dynamics, with anti-vaccine dynamics being treated as a contagion phenomenon [13, 22], and a limited number of studies considered the propagation of both anti- and pro-vaccine behaviour [8, 23]. In addition, researchers have employed a range of techniques to model opinion transmission. For instance, epidemic models have been used in [13, 18, 24, 25], while others have employed opinion diffusion models, such as threshold-based model [11], voter-like model [8], the m-model [23], and a variant of Axelrod's model [22]. The utilization of epidemiological models to describe the spread of opinions provide simple contagion, where an individual can be influenced by a single exposure. In contrast, empirical studies have demonstrated that influence propagation exhibits complex contagion diffusion pattern [26, 27], where multiple exposures are required to influence an individual. Consequently, opinion diffusion models are better suited to capture the dynamics of social interactions, as they incorporate more realistic behavioral characteristics that govern the adoption of opinions and decision-making in the real world.

Anti-vaccine opinion adopters tend to cluster in social networks [19, 28–30]. This leads to the existence of clusters of unprotected individuals which represent a threat to public health and prevent attainment of high vaccination rates [31] as well as impeding the effects of full herd immunity and high vaccination rates [8, 32]. Numerous studies have investigated the risk

of anti-vaccine clusters, focusing for instance on, the relationship between anti-vaccine communities and the epidemic size [8,11,22,28], understanding the communication between vaccine social clusters [30], correlation between spatial clusters and the associated vaccination rates [31], and using social media data to identify vaccine opinion clusters and vaccination rates [28,33,34].

Mitigating the propagation of misinformation has received researchers' attention in the field of influence minimization, which is a subclass of the influence maximization problem. The influence minimization problem focuses on minimizing the propagation of undesirable influence in a social network. Researchers have addressed this problem either by blocking specific nodes [35] or edges [36] in the network, or applying true information campaigns [37–42]. In the context of vaccination hesitancy, empirical research highlights the significance of healthcare providers' advice in overcoming vaccination hesitancy and promoting vaccine uptake through the dissemination of accurate information about vaccines [43,44]. Unlike our main objective, which focuses not only on reducing the number of anti-vaccine opinion adopters but also their distribution in the network to mitigate the growth and connectivity of anti-vaccine communities, existing research on misinformation mitigation has primarily concentrated on single-diffusion processes aimed at reducing negative opinion adopters or increasing positive opinion adopters.

Controlling epidemic spread by managing information dissemination through external campaigns within coupled dynamics is an active research area [22,45,46]. For example, [22] proposed an intervention scheme to control disease spread by governing the spread of anti-vaccine opinions, assuming that agents who adopt anti-vaccine views can be converted back to pro-vaccine views through dedicated influence. Similarly, [45] examined the effects of an intervention campaign aimed at promoting preventive behaviors, specifically by increasing social distancing between agents. A recent study that follows an approach similar to our work [46] investigated the impact of different static targeting heuristics for placing pro-vaccine seeds on epidemic size in a multi-layer setting. Additionally, another study [47] with a similar goal of mitigating vaccine hesitancy proposed strategic targeting methods as a single diffusion process, though it did not consider the effects of these interventions on the dynamics of disease spread.

Although this considerable literature on the dynamics of vaccine-related information and opinion diffusion and their impact on epidemic spread [8,11,18,22,23], several gaps have been identified in the field. First, there is limited consideration of both pro- and anti-vaccine social interactions and preferences that drive epidemic dynamics. Second, there have been limited efforts to address the mitigation of anti-vaccine contagion and its implications for epidemic size through positive campaigns that strategically target individuals to spread positive influence in the network, despite the rich literature on such strategic targeting in other fields such as influence maximization [48,49], misinformation mitigation [37–40], and vaccination strategies [50]. Additionally, despite many studies emphasizing the risk posed by anti-vaccine communities and their correlation with the extent of disease spread, a closer examination of the literature reveals the need for research focused on mitigating the expansion and connectivity of anti-vaccine clusters. Further investigation in these areas could be valuable for advancing our understanding and enhancing our ability to manage and control the spread of diseases.

To bridge these gaps, and with our primary goal of minimizing epidemic size, we develop a computational framework to examine the effects of mitigating anti-vaccine opinions on the size of epidemics, given the correlation between epidemic spread dynamics and the diffusion

of vaccine behaviors. It involves implementation of a strategic counter-campaign that effectively disseminates positive information about vaccines to counteract the diffusion of anti-vaccine opinions. This model integrates vaccine-related information dissemination, pro- and anti-vaccine opinion diffusion, and disease spread. Our main contributions are as follows:

1. We address the mitigation of the diffusion of anti-vaccine opinions as a misinformation mitigation problem, where the primary objective is to seek an optimal set of targets to seed positive influence in a social network. Thus, we explore and compare different heuristics seeking to identify a set of nodes within a network and investigate their effects on the structure of anti-vaccine communities and, ultimately, the extent of disease spread. We examine the impact of various targeting strategies on epidemic size and evaluate the extent to which it can be mitigated.
2. We consider two approaches for the seed set selection: static and dynamic. In the static approach, which has traditionally been considered [37,40,46], the seed set is chosen at the beginning of the campaign launch and remains unchanged throughout the campaign. In contrast, in the dynamic approach, the seed set is selected repeatedly in different rounds based on specific criteria such as [51,52]. We propose a novel dynamic approach where we update the target set with a new target set based on certain criteria. The selection criteria in this approach are based on the local presence of negative vaccine-related information. This is an adaptive approach that responds to the evolving dynamics of the anti-vaccine propagation.
3. We investigate the impact of resource constraints on various network-targeting strategies, highlighting the tradeoff between the number of targeted nodes and the positive influence budget across different campaign types.

Experiments reveal that different methods of distributing positive influence have varying impact on anti-vaccine opinion diffusion and the structure of anti-vaccine communities which consequently affects the epidemic spread. For instance, targeted campaigns demonstrate higher efficiency compared to random campaigns, and the dynamic approach is more efficient than the static approach. Nonetheless, depending on other factors: the allocated positive budget, the level of social influence between individuals, the size of the target set, and the time horizons of dynamic campaigns, we observe variations in the effectiveness of controlling anti-vaccine propagation for each strategy. In the results section, we provide a comprehensive analysis of the performance of each campaign.

Model description and methods

In this study, we consider a scenario where opinion exchanges and the vaccination process occur prior to the spread of the disease. This type of modelling is particularly relevant for diseases like childhood illnesses, e.g., measles, where vaccinations typically take place during the early years of childhood, and the disease manifests during school or preschool age. As a relevant real-world example, in 2019, after almost two decades of significant progress in global vaccination programs, there was a resurgence of measles [53]. One cause of this resurgence is due to a significant decline in vaccine coverage, resulting from the spread of anti-vaccine information.

Motivated by the model presented in [11], we developed a framework consisting of a two-stage agent-based model. The first stage involves opinion diffusion and vaccination processes in relation to individuals' opinions about vaccines, and the second stage is the disease spread among unvaccinated individuals. This modeling approach is a common methodology found in the existing literature on vaccination programs for childhood diseases [8] and

flu-like diseases [3,5,14,54]. We assume that the vaccination provides full immunity, implying that all who receive it are immune to the disease. For vaccine opinion diffusion, motivated by the approach of [11], we developed a model for the dual propagation of positive and negative opinions. Similarly, as in [11], we utilized the SIR model for the disease spread stage, originally developed by [55], which is widely used by researchers in epidemic modeling.

The experiment workflow commences with the stage of opinion diffusion, during which sentiments related to vaccines spread in the network, subsequently influencing individuals' vaccination decision-making. As influenced individuals adopt particular opinions, their social influence starts to propagate through the network. This social contagion inevitably leads to the formation of homogeneous communities, i.e. a community with a particular attitude towards vaccination, with anti-vaccine communities being our primary concern. In our model, we utilize complex contagion, which implies that agents need multiple exposures to be influenced, as this phenomenon has also been observed in influence propagation processes [26,27]. Following the stage of opinion dissemination, the vaccination process takes place. Subsequently, the infectious disease begins to spread among unimmunized individuals. The details of each stage will be explained in the following sections.

We conduct our experiments using the Watts-Strogatz small-world network model [56]. Small-world network provides an effective framework for modelling complex systems, as many real-world networks including social networks [57], exhibit the small-world property [58]. In addition, as the model is stochastic in nature, we conduct a number of simulations per scenario to obtain the average epidemic size. In each simulation, we generate the contact network, followed by the diffusion of opinions and vaccination, and finally the disease spread. An illustration of the model stages is shown in Fig 1.

Opinion diffusion

Our model consists of a network G composed of N nodes, represented by $G(V, E)$, where V is the set of nodes representing individuals, $V = \{1, 2, \dots, N\}$, and E is the set of edges representing contacts between individuals. We assume that this contact structure is the same for both the flow of information and the transmission of the disease. We consider two types of vaccine-related exposures: positive, which spread positive sentiment, and negative, which spread negative sentiment. In addition, we consider exposures from external sources, referred to as general exposure or campaigns, occurring with probabilities μ^- (negative) and μ^+ (positive), as well as through social communication where influence is exerted by opinion adopters on each of their neighbours with probabilities ω^- (negative) and ω^+ (positive), per timestep. Each agent has their own set of counters $\{\phi^-, \phi^+\}$, where ϕ_i^- quantifies exposures to negative, and ϕ_i^+ quantifies exposures to positive sentiments experienced by each agent. Furthermore, θ is an opinion decision threshold that represents an individual's sensitivity to influence. We assume that an agent shifts its opinion from a neutral state to either negative or positive when it has been exposed to θ more exposures of a particular influence.

Each agent i , $i = \{1, 2, \dots, N\}$, may adopt one of three opinion states $s_i \in \{o^-, o^0, o^+\}$, where o^- is negative, o^+ is positive, and o^0 is neutral. We assume that once an agent changes its state from a neutral to a negative (or positive) state, it remains in that state, as we assume that individuals with a pro-vaccine opinion choose to immunize, achieving full immunity, while anti-vaccine individuals refuse vaccination and maintain their stances. This is consistent with real-world observations of the growing polarization in the vaccine debate, driven by misinformation and social media echo chambers, which reinforce entrenched views [59,60], making stances changes less likely. To summarize, following a setup informed by the approach taken in [11], our model operates in discrete time steps as follows:

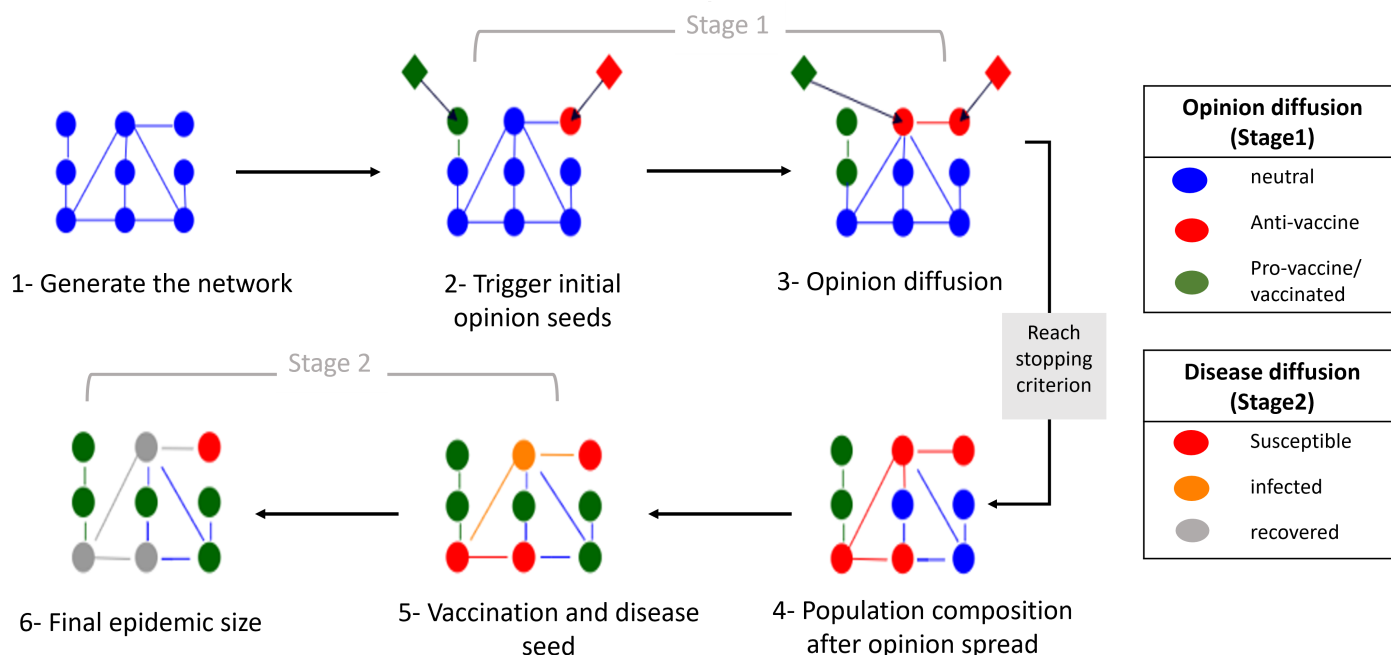


Fig 1. Illustration of the model describing opinion formation and disease propagation. Blue circles represent neutral individuals, green circles represent pro-vaccine individuals, and red circles represent anti-vaccine individuals. The first stage involves the generation of the social network and the initialization of agent opinion states as agents with neutral opinions. Then, external exposures to positive and negative information triggers the initial seed sets for both anti-vaccine and pro-vaccine contagion. Opinion diffusion continues until a stopping criterion is reached. In this stage, a vaccination takes place for all non-negative individuals. Subsequently, a randomly chosen non-vaccinated individual is infected, and the spread of the disease continues until no further newly infected agents are generated. Finally, we record the number of recovered agents to measure the epidemic size.

<https://doi.org/10.1371/journal.pone.0318544.g001>

- At time $t = 0$, all agents are neutral, i.e., $s_i = o^0, \forall i \in V$.
- At each time step t , negative general exposure exerts influence on the population with probability μ^- per individual. Similarly, positive general exposure exerts influence on the targeted population with probability μ^+ per individual. In addition, each agent i with state $s_i \in \{o^-, o^+\}$, exerts influence on each of its neutral neighbors with probability ω^- for negative opinion adopters and ω^+ for positive opinion adopters. Exposures for an agent i , i.e., $\{i \in V | s_i = o^0\}$, is added to ϕ_i^- if it is negative or added to ϕ_i^+ if it is positive.
- At each time step t , each neutral agent i , i.e., $\{i \in V | s_i = o^0\}$, updates its opinion state as follows:

$$s_i = \begin{cases} o^- & \text{if } \phi_i^- - \phi_i^+ \geq \theta, \\ o^+ & \text{if } \phi_i^- - \phi_i^+ \leq -\theta, \\ o^0 & \text{otherwise.} \end{cases} \quad (1)$$

The above process is repeated for τ steps. A visual depiction of external campaigns and social influence is shown in Fig 2A. Next, we make the assumption that all agents with a non-negative opinion will receive the vaccine, while those with a negative opinion will refuse it.

Epidemic spread

In this phase, an anti-vaccine opinion adopter is randomly chosen as a seed for the disease, and disease spread is modeled using the SIR model. Each infected agent can transmit the

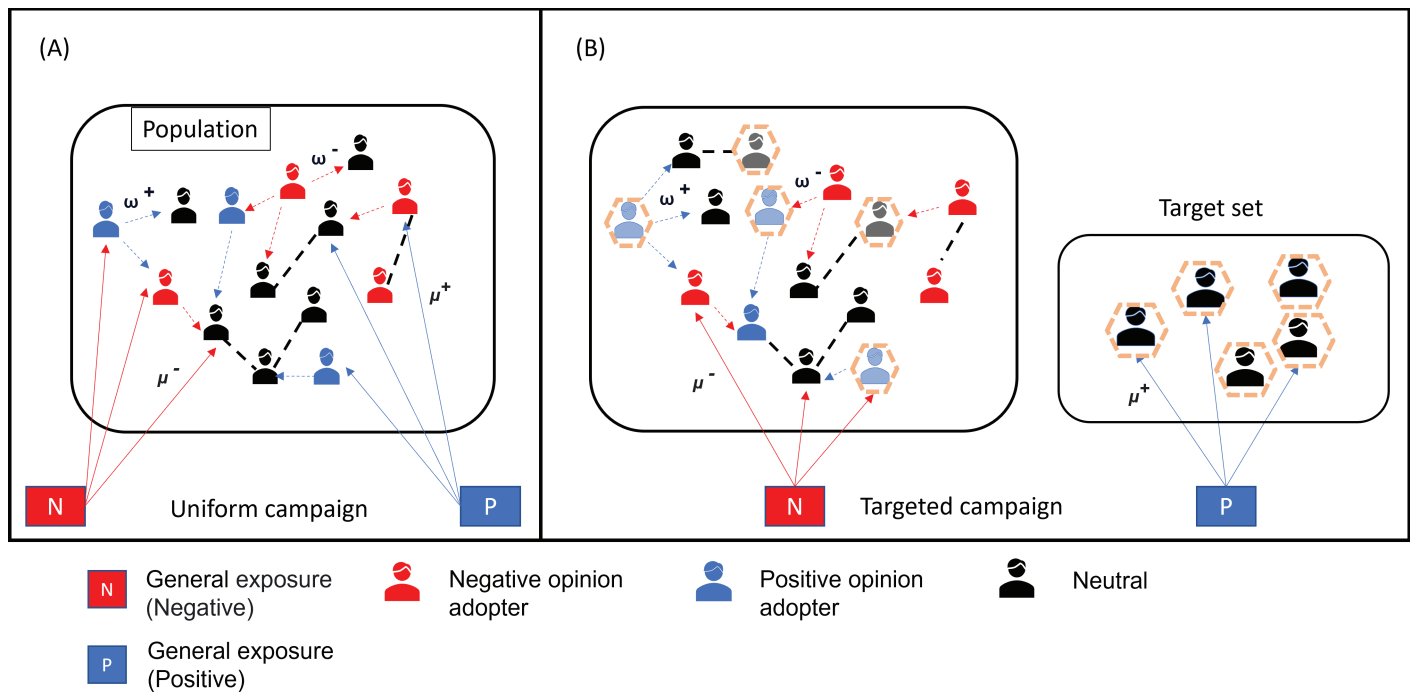


Fig 2. Illustration of opinion propagation and campaigning methods. The figure shows the exchange of vaccine-related opinions and external exposures, as well as the positive campaign types. (A) Random dissemination of negative and positive vaccine-related sentiments from external campaigns to the public. (B) Targeted positive campaign. μ^- , and μ^+ are the general exposure rates for negative and positive sentiments, respectively. ω^- , ω^+ are the social exposure rates for negative and positive opinions, respectively.

<https://doi.org/10.1371/journal.pone.0318544.g002>

disease with a probability β per contact per time step, and can recover with a probability γ per time step. The process continues until there are no more infected individuals, and the epidemic size S_r is recorded. S_r is defined as the total number of individuals who experience an infection during the course of the epidemic [61].

Table 1 below presents a list of the model parameters and their corresponding descriptions.

Campaign strategies

In this study, we define a positive campaign as a strategic allocation of the strength of positive external vaccine information, denoted as μ_i^+ , to the agents $i = 1, \dots, N$, with $1/N \sum_i \mu_i^+ = \mu^+$. We compare the effectiveness of various types of such positive campaigns against a random negative campaign that spreads negative vaccine information, assuming that each agent can be negatively influenced with an influence strength $\mu_i^- = \mu^-$ at each time step. This section outlines the proposed selection strategies for the target set for the positive campaign. Table 2 below provides an overview of the proposed strategies.

Random campaign (StatRandAll)

In this scheme, we extend the work introduced by [11], in which they explored the impact of only anti-vaccine opinions on the formation of anti-vaccine communities. In their model, all individuals can be influenced by a general negative exposure with a specific rate. In our

Table 1. Model parameters and descriptions.

Parameter	Parameter Description
N	Population size
μ^-	Negative general exposure rate
μ^+	Positive general exposure rate
ω^-	Negative social rate
ω^+	Positive social rate
ϕ^-	Negative exposure counter
ϕ^+	Positive exposure counter
θ	Opinion formation threshold
T	Target set size
t_r	Update time interval for the dynamic control
τ	Opinion diffusion time steps (stopping criterion)
ζ	Target number of anti-vaccine neighbours
Z	Target number of neutral neighbours
β	Disease infection rate
γ	Disease recovery rate
I_0	Initial number of infected individuals
S_r	Epidemic size

<https://doi.org/10.1371/journal.pone.0318544.t001>

Table 2. Campaign strategies and descriptions.

Campaign type	Campaign name	Acronym	Description
Baseline	Random	StatRandAll	All agents can be influenced with a uniform positive allocation μ^+ at each time step.
Static	Targeted random	StatRandT	An unchanged random subset of the entire population.
	Centrality-based	StatCentT	The T most central agents in the network.
Dynamic	Dynamic random	DynRandT	A random subset of the entire population, which is replaced with a new target set at random every t_r .
	Local information based	DynAntiT	Agents who have at least one anti-vaccine neighbor.
	Advanced Locl-Info with single-objective	DynLocT	The T agents with the lowest score according to the number of adjacent anti-vaccine neighbors, Eq 2.
	Advanced local-info with multi-objective	DynAdvLocT	The T agents with the lowest score according to the number of adjacent anti-vaccine and neutral neighbors, Eq 3.

<https://doi.org/10.1371/journal.pone.0318544.t002>

baseline campaign, all individuals are also exposed to a positive exposure, with a positive allocation $\mu_i^+ = \mu^+$ at each time step. The campaign scheme is illustrated in Fig 2(A).

Targeted campaigns

In this approach, we aim to target a certain set of agents with neutral opinions, as illustrated in Fig 2(B), to efficiently mitigate the spread of anti-vaccine influence. This puts a greater emphasis on specific individuals and has been demonstrated as an effective method, as evidenced by empirical studies [62]. There are several ways to target them: (i) random selection as a common and intuitive approach; (ii) based on their topological position on the network; (iii) based on their neighbourhood status with regards to local information about vaccine opinions. Each of these will be explained in detail in the subsequent sections.

Furthermore, this approach involves two types of campaigning: static and dynamic. In the static approach, the target set is selected based on predetermined criteria prior to the launch

of the campaign and this set remains unchanged. In the dynamic approach, the initial targets are selected at random, however, every t_r opinion updates the target set is updated and replaced by new targets.

In the targeted approach, let $T_i = 1$ if agent i is targeted and $T_i = 0$ otherwise. Accordingly, the positive campaign allocation $\mu_i^+ = T_i \times \mu^+ \times N / \sum_i T_i$. This campaigning scheme directs the positive influence budget toward specific individuals rather than distributing it across the entire population, optimizing resource use and increasing the allocation dedicated to targeted individuals. In the following, we have explored and compared the following six heuristics for selecting the target set.

Static campaigns. The following strategies outline the criteria for selecting the target set in the static campaign approach.

1. **Targeted random strategy (StatRandT):** a random subset of the entire population is selected as the campaign's targets.
2. **Targeted centrality-based strategy (StatCentT):** this is a topology-based campaign in which targets are selected based on betweenness centrality. The T most central agents in the network are targeted. In the case of ties among agents with the same score, we randomly select T agents from among the tied nodes. We compute the betweenness centrality score for each agent following the algorithm proposed by [63]. Betweenness centrality measures the extent to which a node lies on the shortest paths between other nodes in the network [64]. Nodes with high betweenness centrality are considered to be mediators [65] and are often located on important bridges in the network, making them key players for information flow and communication. Targeting these nodes can potentially have a greater impact on the overall network dynamics, creating barriers for anti-vaccine communities and preventing them from merging together. We explored additional centrality measures but found very limited differences (see Fig 1 in [S1 Appendix](#) for a comparison). For this reason, in the remainder of the paper we will only consider betweenness centrality.

Dynamic campaigns. Dynamic campaign strategies rely on the local information about individuals' opinions regarding vaccines. Targeting based on neighborhood information has previously been utilized in other fields, including cooperation in multi-agent systems [66] and minimizing negative diffusion (e.g., [52]). The following strategies outline the criteria for selecting the target set based on this information.

1. **Dynamic random strategy (DynRandT):** at each time interval t_r , the target set is replaced with a new target set by selecting from the remaining population of agents with neutral opinions at random. We consider this campaigning strategy as a reference to evaluate the effectiveness of other dynamic selection criteria.
2. **Dynamic local information based strategies:** in this approach, our objective is to focus on agents with neutral opinions who are susceptible to negative influence from their social connections, i.e., agents with neutral opinion who have at least one anti-vaccine neighbour. This is a neighborhood-based scheme with two primary considerations: first, placing seeds to effectively inhibit the growth of the negative cluster, which requires them to have a certain number of negative neighbors; second, situating positive seeds in a way that maximizes the potential for positive clusters to grow (and eventually block negative clusters), which means targeting neutral agents with the greatest number of neutral neighbors. We expect a trade-off here. If agents have too many negative neighbors, they may become overwhelmed quickly, and thus positive influence

might be wasted. Contrariwise, targeting agents with too many neutral neighbors might place them too far from negative clusters, thus becoming inefficient at blocking negative clusters from growing. We formalise this trade-off as follows:

- i. **Local information based (DynAntiT)**: at each time interval t_r , the target set is updated and replaced with a new target set by selecting at random from the remaining population of agents with neutral opinions who have at least one anti-vaccine neighbor.
- ii. **Advanced Local-Info with single-objective (DynLocT)**: Here, we aim to target neutral agents who are in neighbourhoods that meet a trade-off between blocking negative influence and allowing positive influence to spread. The first is related to the number of adjacent negative agents and the second relates to the number of adjacent neutral agents. Let ζ be the target number of anti-vaccine neighbours, here, we seek to target neutral agents who have as close as possible to ζ . In more detail, we do this by scoring agents according to the difference in their number of anti-vaccine neighbours from ζ as follows:

$$g_i(\zeta) = |n_i^- - \zeta|, \quad (2)$$

where n_i^- denotes the actual count of anti-vaccine neighbours for an agent i . Then, we select the T agents with the lowest score (and selecting at random in case of ties). If the number of agents selected is less than T , the selection process continues by choosing from the remaining population of agents with neutral opinions at random until T agents have been selected. We will vary ζ to identify the heuristic that best suppresses disease outbreaks.

- iii. **Advanced local-info with multi-objective (DynAdvLocT)**: This heuristic builds on the previous heuristic, but we now also include the potential for positive information to spread by including the number of neutral neighbours in the scoring process. Again, let ζ be the target number of anti-vaccine neighbours and Z be the target number of neutral neighbours of an agent. Next, presuming that agent i has n_i^- anti-vaccine neighbours and n_i^0 neutral neighbours, we calculate a score according to:

$$g_i(\zeta, Z) = |n_i^- - \zeta| + |n_i^0 - Z|, \quad (3)$$

and select the T agents with the lowest scores. In the case of ties among agents with the same score, we randomly select T agents from among the tied nodes. If the number of agents selected is less than T , the selection process continues by choosing from the remaining population of agents with neutral opinions at random until T agents have been selected. Below we will explore the dependence of the effectiveness of the heuristic on both target numbers of negative neighbours ζ and neutral neighbours Z .

Results

In this section, we present the obtained epidemic size for the proposed positive campaigns. During the first stage, i.e., opinion exchanges, we consider two cases as stopping criteria: one where opinions spread until all agents have adopted an opinion, referred to as $\tau = \infty$, which represents the long-run scenario and enables the evaluation of the long-term behavior. The other scenario where opinions spread over a certain period of time τ , represents the short-run scenario. In the short-run case, we compared the obtained epidemic size with that from a scenario where only anti-vaccine opinion diffusion is considered, previously investigated in [11]. While our experimental setting differs from that of [11], we have applied their work within

our setting for comparison purposes. We conducted extensive experiments to investigate the factors that determine the efficacy of each campaign in promoting vaccination.

Unless otherwise stated, the results show the epidemic size as a function of the social contagion rate parameter ω to compare the varying strengths of social influence on vaccine decision-making and their impact on the emergence of anti-vaccine communities and consequently disease spread. The social rate is a crucial component because it controls the growth of anti- and pro-vaccine communities. A low social rate implies that individuals are barely influenced by their social contacts, resulting in a low growth of anti-vaccine communities. In contrast, a high social rate indicates that individuals are highly influenced by their social contacts, leading to a large growth of anti-vaccine communities. To simplify the analysis, we have assumed equal social rates for pro- and anti-vaccine diffusion and evaluated the impact of different rates of positive general exposure μ^+ on the epidemic size, while keeping the negative general exposure μ^- fixed. The shaded area and error bars represent the 95% confidence intervals. Due to the small error values and the large y-axis scale, the shaded confidence interval area might not be clearly visible in some figures.

In all experiments, following a configuration similar to that used in [11], we consider a small-world network with size $N = 5000$, rewiring probability $p = 0.01$, average degree $\langle k \rangle = 10$, and the social rate range $\omega^- = [10^{-4}, 10^{-2}]$. We use an opinion formation threshold of $\theta = 2$ as we consider complex contagion. For the SIR parameters, also following [11], we set the infection rate $\beta = 0.1$, recovery rate $\gamma = 0.1$, and seed set $I_0 = 1$. For the general negative exposure rate (μ^-), we consider a value of 0.001, chosen to be close to the positive influence μ^+ . For the additional parameters introduced in this study, specifically (μ^+ , ω^+ , T , t_r , ζ , Z), we have investigated the sensitivity to each. Unless otherwise stated, for each scenario we generate 500 different networks and for each network we run 500 SIR infection simulations.

Results of the random campaign (StatRandAll)

This section presents the epidemic size obtained by applying the random campaign to disseminate positive vaccine-related information, as illustrated in Fig 3.

Fig 3A illustrates the long-run scenario with $\tau = \infty$ for varying social rates. This campaign seeds positive influence widely by targeting the whole population at random, resulting in a large number of seeds being generated, with the same occurring for negative seeds. When the social rate ω is low (e.g., $\omega < 10^{-3}$ in Fig 3A), the social influence of these seeds is slow, resulting in unconnected and smaller homogeneous communities, namely anti-vaccine and pro-vaccine communities. In addition, the existence of pro-vaccine communities prevents the merging of anti-vaccine communities. This ultimately leads to a smaller epidemic size compared to a higher social rate.

In contrast, when the social rate is high (e.g., $\omega = 10^{-2}$ in Fig 3A), the social influence of these seeds spreads rapidly, leading to fast expansion of the communities and allowing merging of communities. In this scenario, due to the rapid diffusion of opinions, the positive campaign fails to exert more influence over time, as the majority of individuals have already adopted an opinion. This ultimately results in large-sized communities and subsequently a higher epidemic size within anti-vaccine communities. This pattern is observable when the negative and positive general exposure rates diffuse at nearly equal rates, represented by red and light-blue lines in the figure. Nevertheless, with a much lower positive general exposure rate $\mu^+ \ll \mu^-$ (dark-red line), this pattern is almost nonexistent, since the positive seeding rate is low, rendering the negative influence dominant regardless of the social rate. In contrast, when the positive rate is much greater than the negative rate $\mu^+ \gg \mu^-$, represented by

blue and dark-blue lines, the epidemic size dramatically decreases to less than 50 at the lowest social rate, i.e., $\omega = 10^{-4}$. Although the social rate does not play a significant role in such scenarios, higher social rates, namely $\omega = 10^{-2}$, lead to an increase in the epidemic size to less than 500.

Moreover, an increase in the positive external rate μ^+ results in a decrease in the epidemic size. The disparity in budget allocations for negative and positive external rates plays a pivotal role in shaping the prevalence of anti-vaccine opinions. A higher positive external rate than negative external rate leads to a dominance of positive influence, resulting in a smaller number of anti-vaccine opinions and consequently a smaller epidemic size, and vice versa.

Fig 3B gives results for $\tau = 400$, and allows for a comparison between scenarios with and without positive campaigns. The figure distinctly illustrates that the propagation of positive vaccine-related information always yields a positive effect, resulting in a reduction in epidemic size compared to the scenario in which only anti-vaccine opinions are being spread (green line). Furthermore, the suppression of the epidemic increases as the positive general exposure rate μ^+ increases. However, as the social rate increases, the growth of communities also increases, leading to a higher epidemic size.

Results of the static campaigns

This section presents the epidemic size obtained by using targeted static campaigns to disseminate positive vaccine-related information. This includes the targeted random and targeted centrality-based campaigns.

Fig 4A and 4C illustrate the long-run scenario with $\tau = \infty$ for the targeted random and centrality-based campaigns, respectively. In general, the centrality-based campaign performs better in reducing the epidemic size than the targeted random campaign. Additionally, as the positive rate μ^+ increases, the performance of the campaigns improves, leading to higher

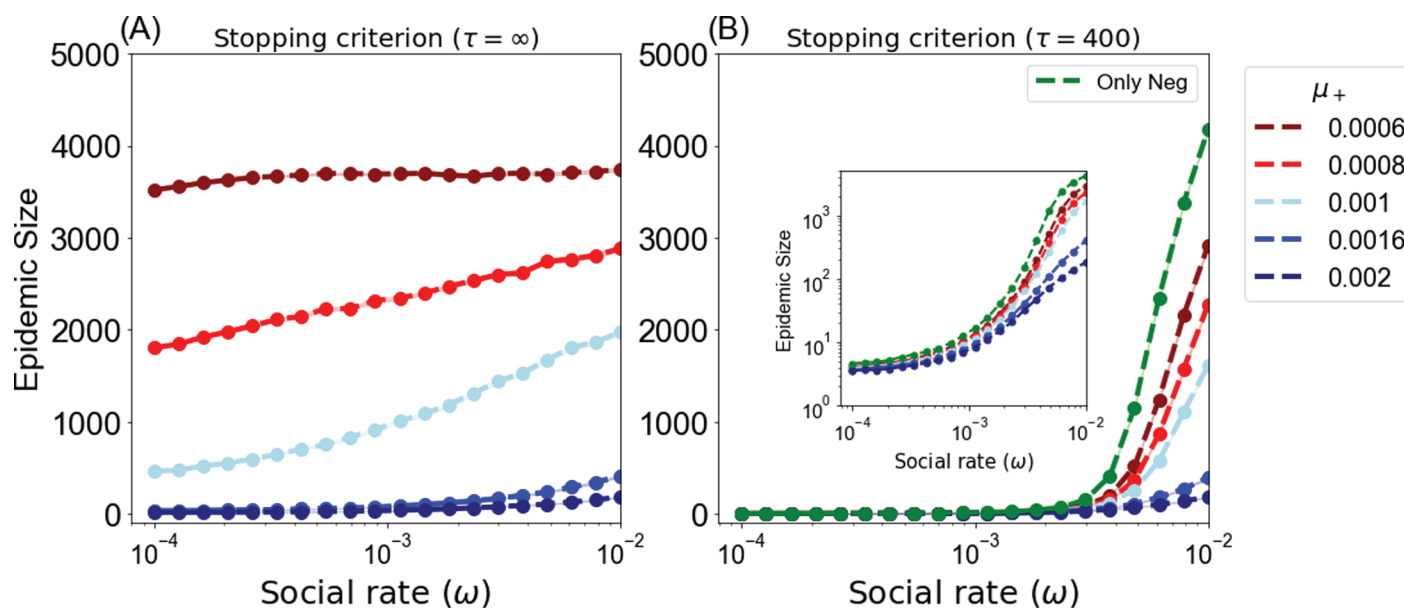


Fig 3. Average epidemic size for the random campaign (StatRandAll) as a function of the social rate $\omega = \omega^+ = \omega^-$. (A) $\tau = \infty$ (B) $\tau = 400$. The figure shows results for different positive exposure rates μ^+ with fixed negative exposure rate $\mu^- = 0.001$.

<https://doi.org/10.1371/journal.pone.0318544.g003>

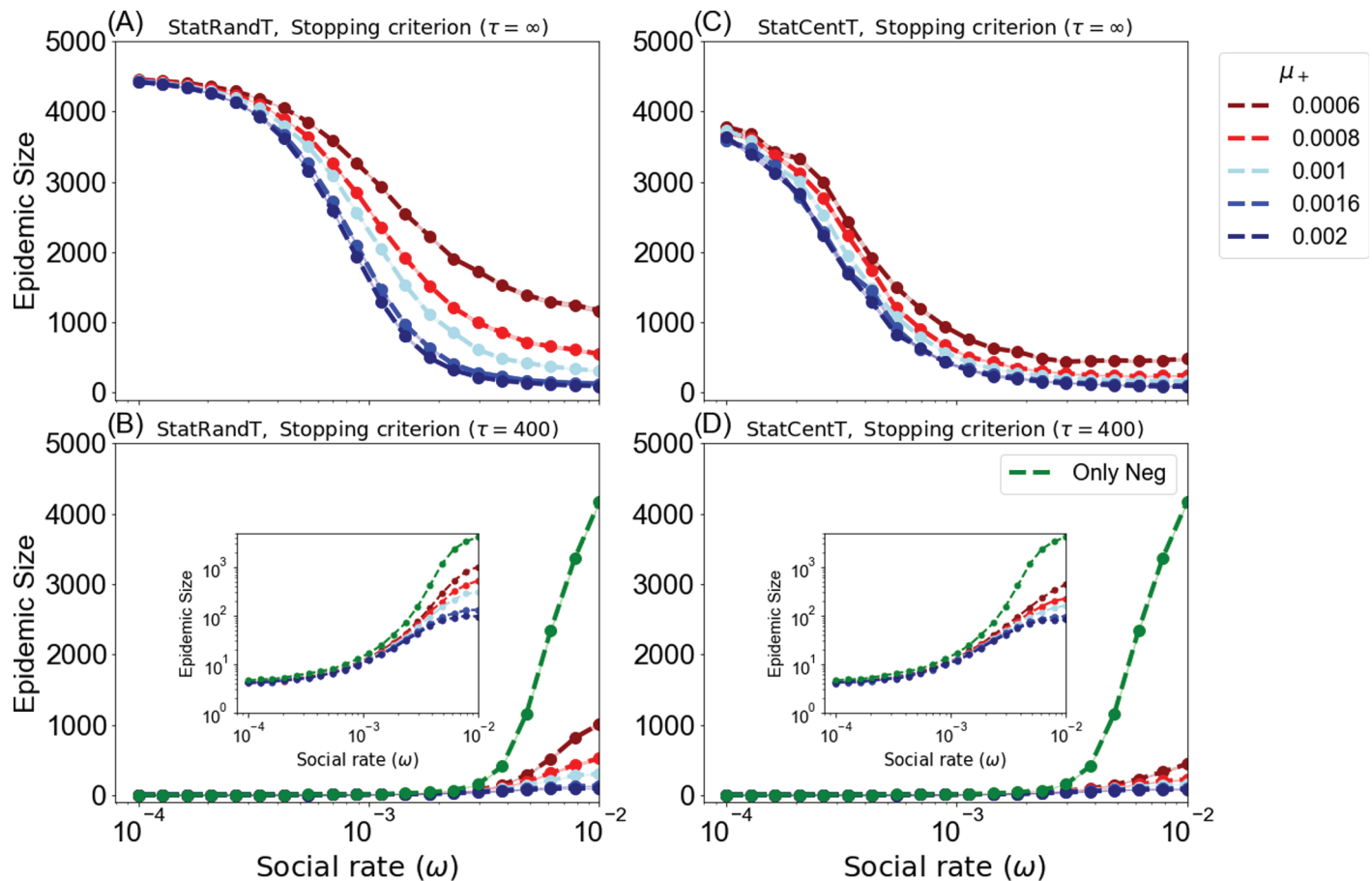


Fig 4. Average epidemic size for static campaigns as a function of the social rate $\omega = \omega^- = \omega^+$. (A) and (B) for the targeted random campaign (StatRandT). (C) and (D) for the centrality-based campaign (StatCentT). (A) and (C) $\tau = \infty$, (B) and (D) $\tau = 400$. The figures show different positive exposure rates μ^+ with fixed negative exposure rate $\mu^- = 0.001$. Target set size is $T = 500$. For each scenario we generate 300 different networks, and perform 300 SIR model runs for each network.

<https://doi.org/10.1371/journal.pone.0318544.g004>

epidemic suppression. However, for the centrality-based campaign, this improvement is relatively small due to the fact that this campaign is efficient even when positive exposure rates are low.

More importantly, there is a notable difference between the random (StatRandAll) and targeted campaigns in regard to the social influence rate ω . When the social rate is low, individuals tend to exchange opinions less frequently, and their vaccination behavior is largely influenced by the external campaigns. This is shown clearly in the long-run setting, where all individuals adopt a vaccine opinion, as seen in Figs 3A, 4A, and 4C. Under these circumstances, the random campaign, see Fig 3A, tends to yield a smaller epidemic size compared to static campaigns, see Fig 4A, 4C. This is due to the fact that the random campaign generates a larger number of positive seeds over time than the targeted campaigns, which are restricted to a fixed set of agents. With lower levels of social interaction, the growth of homogeneous communities is slower, resulting in the formation of a large number of small, unconnected communities. More importantly, the scattered spread of positive seeds prevents mergers between the anti-vaccine communities. As a consequence, these smaller communities yield a smaller epidemic size.

In contrast, targeted campaigns generate limited seeds as they work with a specific and static target set and not the entire population, so their impact is restricted to the positions of these seeds. In the centrality-based campaign, these positions are the most central nodes in the network, and as a result, they behave better in reducing the epidemic as they efficiently mitigate the connectivity between anti-vaccine communities compared to the targeted random campaign, where the target set is chosen at random.

On the other hand, when the social rate is high, targeted campaigns work better in containing the disease dynamics, resulting in smaller epidemic size as the strategically positioned targets reduce the connectivity between the anti-vaccine communities.

To further explain, consider the scenario where $\mu^- = \mu^+$, represented by light-blue curves. In the random campaign shown in Fig 3A, the epidemic size increases as the social rate ω increases. However, the targeted random (StatRandT) and targeted central campaigns (StatCentT) shown in Fig 4A and 4C, respectively, exhibit an inverse behavior, with the epidemic size decreasing as the social rate increases. The reason for this is that with broad seeding and less social interaction, the seeds act as obstacles distributed across the network, efficiently mitigating the merging between anti-vaccine communities. However, with a limited number of targets in the targeted campaign and a low rate of social interaction, these campaigns fail to mitigate the propagation of anti-vaccine influence, which is reinforced by broad and continuous exposures, as their effect only associates with their positions. On the other hand, with higher social rates, opinions are diffused faster, making it challenging to exert more influence over time. Thus, the random campaign becomes less efficient compared to the targeted campaign, where the fixed positions of the targets successfully impede the connectivity of the anti-vaccine communities. The same behavior is observed regardless of the size of the positive campaign budget μ^+ .

Furthermore, Fig 4B and 4D display the system at time $\tau = 400$, allowing for a comparison between the campaign and the anti-vaccine opinion only scenario for the targeted random and centrality-based campaigns, respectively. The figure distinctly illustrates that the propagation of positive vaccine-related information results in a positive effect. As demonstrated in the figures, this approach reduces the epidemic size when compared to the scenario where only anti-vaccine opinions exist. Furthermore, the suppression of the epidemic increases as the positive general exposure rate increases. However, as the social rate increases, the growth of communities also increases, leading to a higher epidemic size.

A noteworthy observation is that the centrality-based campaign (StatCentT) is more effective in reducing the epidemic size than random campaigns compared to the scenario where only anti-vaccine opinions are spread. Additionally, the targeted random campaign (StatRandT) is more effective than the random campaign (StatRandAll). For instance, consider the scenario where $\mu^+ = \mu^-$, as shown by the light-blue lines in Figs 3B, 4B, and 4D. At the highest social rate, i.e., $\omega = 10^{-2}$, the epidemic size for the random (StatRandAll), targeted random (StatRandT), and centrality-based campaigns (StatCentT) is 1615 ± 27 , 302 ± 13 , and 161 ± 5 , respectively, compared to 4174 ± 15 for the scenario where only anti-vaccine opinions are being spread.

Results for the dynamic campaigns

This section presents the epidemic size obtained by applying targeted dynamic campaigns to disseminate positive vaccine-related information. This includes the dynamic random (DynRandT) and dynamic local information-based (DynAntiT) campaigns.

Fig 5 displays the results obtained by these campaigns. We evaluate the campaigns for different update times and results are presented as a function of the target set update time

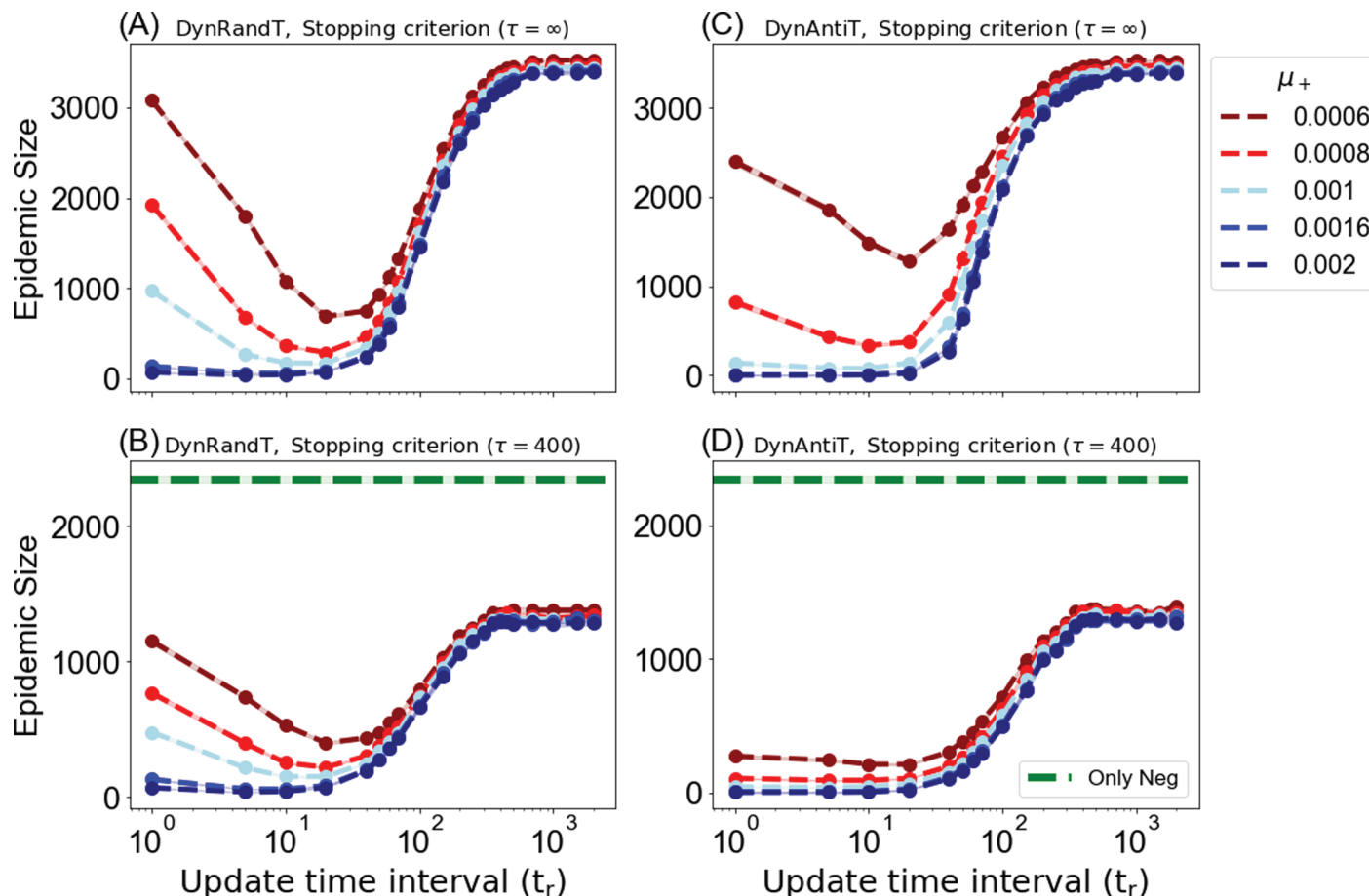


Fig 5. Dependence of the average epidemic size on the campaign updating interval using dynamic campaigns. (A) and (B) represent the dynamic random campaign DynRandT, and (C) and (D) represent the DynAntiT campaign. (A) and (C) $\tau = \infty$, (B) and (D) $\tau = 400$. The targets set $T = 50$, social rate is $\omega^+ = \omega^- = 0.006$. The figures show different positive exposure rates μ^+ with fixed negative exposure rate $\mu^- = 0.001$.

<https://doi.org/10.1371/journal.pone.0318544.g005>

interval t_r . Here if the target set is changed very often, since multiple exposures are required for adopting opinions, the likelihood of each individual agent being influenced is very low. Correspondingly, fairly small amounts of influence are spread over a large set of agents that are targeted at different times. In contrast, when leaving the target set unchanged for longer, agents in the target set can accumulate multiple exposures which might lead to opinion adoption. However, this also implies that influence is not spread very widely and occasionally agents who already hold an opinion might be targeted. From these considerations it becomes clear that there must be an optimal switching time which maximizes the effect of the positive campaign.

Fig 5A and 5C illustrate the long-run scenario with $\tau = \infty$ for varying update time intervals for the dynamic random DynRandT and DynAntiT campaigns, respectively. The results demonstrate that an optimal update time interval exists at around $t_r = 20$. This is particularly obvious when the general positive exposure rate μ^+ is lower than the negative one $\mu^+ \ll \mu^-$. This optimal time results from the trade-off explained above. Therefore, with a lower general positive exposure rate, the campaign performs better with relatively slow updates.

On the other hand, as the general positive exposure rate increases, indicating a stronger positive influence, the pronounced effect—i.e., an optimal time at $t_r = 20$ —diminishes. This effect becomes almost negligible when $\mu^+ > \mu^-$ in the DynRandT campaign, and when $\mu^+ \geq \mu^-$ in the DynAntiT campaign. In such cases, the fastest update strategy $t_r = 1$ becomes an effective option. This phenomenon occurs because a higher general positive exposure rate increases the probability of positive influence, and when combined with quick updates, it allows us to attain widespread coverage by targeting susceptible agents before they are negatively influenced. Moreover, after a time interval of $t_r = 10$, the epidemic size continues to increase as the interval t_r increases until reaching a stationary state, where there are no further changes in the epidemic size. As we increase the update intervals, we reduce the scope of our targeting coverage, resulting in a corresponding decrease of the positive effects we initially achieved in mitigating the negative influence.

Furthermore, comparing the DynRandT and DynAntiT campaigns, Fig 5A and 5C demonstrate varying performance in reducing the spread of an epidemic. For the smallest positive general exposure rates displayed in the figure, e.g., dark-red lines and $\mu^+ = 0.0006$, which is much smaller than the negative general exposure rate $\mu^- = 0.001$, the dynamic random strategy outperforms the DynAntiT strategy at the optimal time $t_r = 20$, resulting in a smaller epidemic size. At time $t_r = 20$, the epidemic size is 1276 ± 29 and 688 ± 19 with $\mu^+ = 0.0006$, and 375 ± 13 and 288 ± 8 with $\mu^+ = 0.0008$ for DynAntiT and dynamic random DynRandT, respectively. However, as the general positive exposure rate increases, the DynAntiT strategy is more effective at mitigating the negative influence. This is also noticeable when both positive and negative rates spread at the same rate, i.e., $\mu^+ = 0.001$, where epidemic size at time interval $t_r = 1$, is 139 ± 8 and 972 ± 23 for DynAntiT and dynamic random, respectively. Furthermore, the epidemic size reduced even further when the positive general exposure rate was much greater than the negative rate with $\mu^+ = 0.002$ and $\mu^- = 0.001$ and reached 3 ± 0.08 and 70 ± 2 for the DynAntiT and dynamic random campaigns respectively, at $t_r = 1$.

Fig 5B and 5D display the system at time $\tau = 400$ for the dynamic random and DynAntiT campaigns, respectively, allowing for a comparison between the campaigns and the only anti-vaccine opinion scenario. Once again, the dissemination of positive vaccine-related information yields a positive impact in mitigating the diffusion of anti-vaccine sentiments compared to the scenario where only anti-vaccine opinions are disseminated. Furthermore, the suppression of the epidemic increases as the positive general exposure rate increases.

Results for the advanced local-info campaigns

This section presents the epidemic size obtained when applying the advanced targeted dynamic campaigns to disseminate positive vaccine-related information. This includes the targeted advanced local-info (DynLocT) and multi-objective advanced Local-Info (DynAdvLocT) campaigns. For the DynLocT campaign, the results are presented as a function of the target number of anti-vaccine neighbors ζ to assess the impact of this parameter on mitigating the growth of anti-vaccine communities and, consequently, reducing the size of the epidemic. For the DynAdvLocT campaign, the results are presented as a function of both ζ and Z , with different values of μ^+ to explore the trade-off between maximizing the growth of pro-vaccine communities and minimizing the growth of anti-vaccine communities. The results are shown in Figs 6 and 7 for DynLocT and DynAdvLocT campaigns, respectively.

For DynLocT campaign, considering the long-run behavior with $\tau = \infty$, see Fig 6A, we found that optimal performance is obtained for $\zeta \leq 1$, which is particularly obvious when the

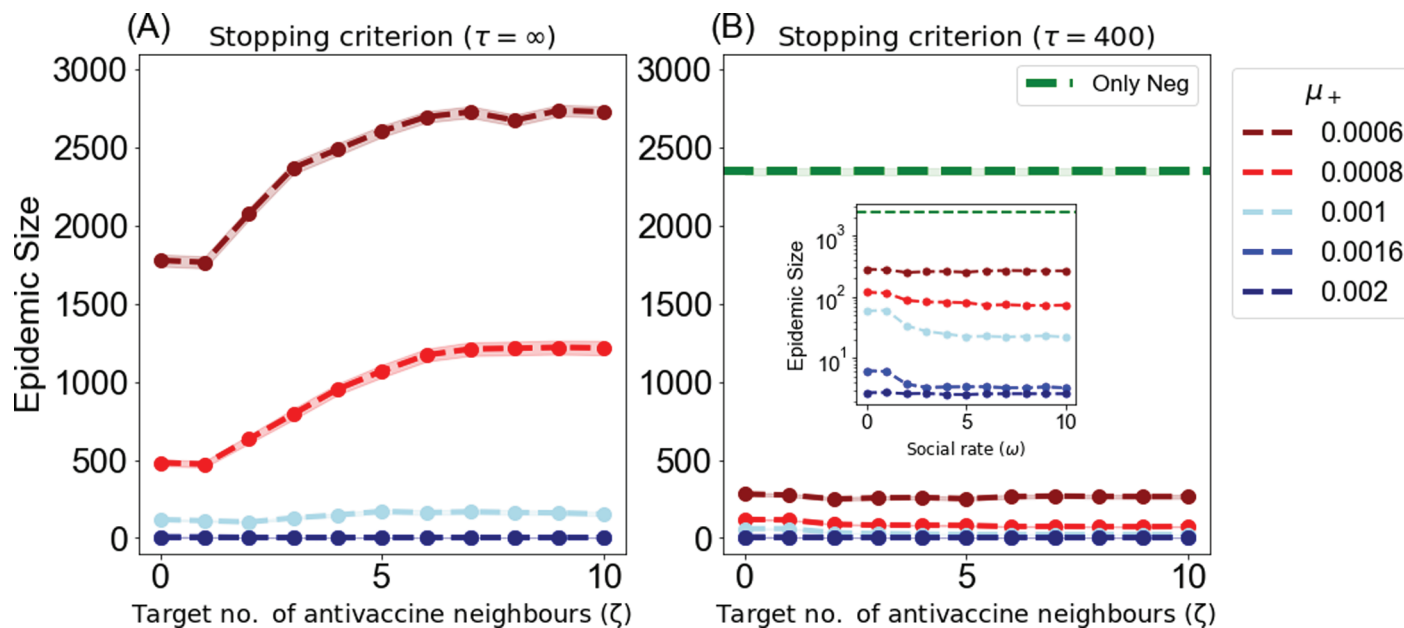


Fig 6. Dependence of the average epidemic size on the target number of anti-vaccine neighbors ζ using the DynLocT campaign. The updating time is $t_r = 1$, the social rate is $\omega = 0.006$ for both negative and positive $\omega^+ = \omega^-$, and the size of the target set is $T = 50$. The figures show different positive exposure rates μ^+ with fixed negative exposure rate $\mu^- = 0.001$.

<https://doi.org/10.1371/journal.pone.0318544.g006>

positive rates μ^+ are significantly lower than the negative rates μ^- , as indicated by the dark-red line in the graph. We also observed the same behavior found in the dynamic campaigns, where fast updates with weak influence rates are not effective in convincing the target set before they are updated since agents require multiple exposures to adopt a particular opinion. The challenge becomes greater when selecting neutral agents who are surrounded by many anti-vaccine adopters, as they are more likely to be negatively influenced by their social contacts. However, this behavior diminishes as the positive influence rate increases and leads to a significant reduction in the epidemic size, particularly when $\mu^+ \gg \mu^-$, regardless of the ζ value. For example, the epidemic size remains the same at $\zeta = 1$ and $\zeta = 8$, taking a value of 3 ± 0.1 , see Fig 6A at $\mu^+ = 0.002$.

In the case of the DynAdvLocT campaign, similar to DynLocT, we have observed that an optimal reduction in the epidemic size is obtained for $\zeta \leq 1$, particularly when the positive rates μ^+ are considerably lower than the negative rates μ^- , as depicted in Fig 7A. Moreover, this reduction increases as Z increases, indicating a focus on targeting individuals with a larger number of neutral neighbors. However, there is a remarkable observation that when $Z \geq 10$, the epidemic size is significantly diminished irrespective of the ζ value, which is equivalent to the average degree of the network $\langle k \rangle = 10$. Furthermore, when $Z > 10$, the epidemic size remains relatively constant.

Furthermore, in the case of $\mu^+ = \mu^-$, as shown in Fig 7B, a more significant reduction in the epidemic size is observed with fewer target number of neutral neighbours Z compared to the previous scenario. The figure indicates that we can achieve a greater reduction when $Z > 7$. As an example, this campaign efficiently reduced the epidemic size to 12 ± 0.5 when $\zeta = Z = 10$. Furthermore, beyond this point, this reduction remains relatively constant, and increasing the Z value does not yield any additional effect. In this scenario, the number of anti-vaccine neighbors, does not have a major effect.

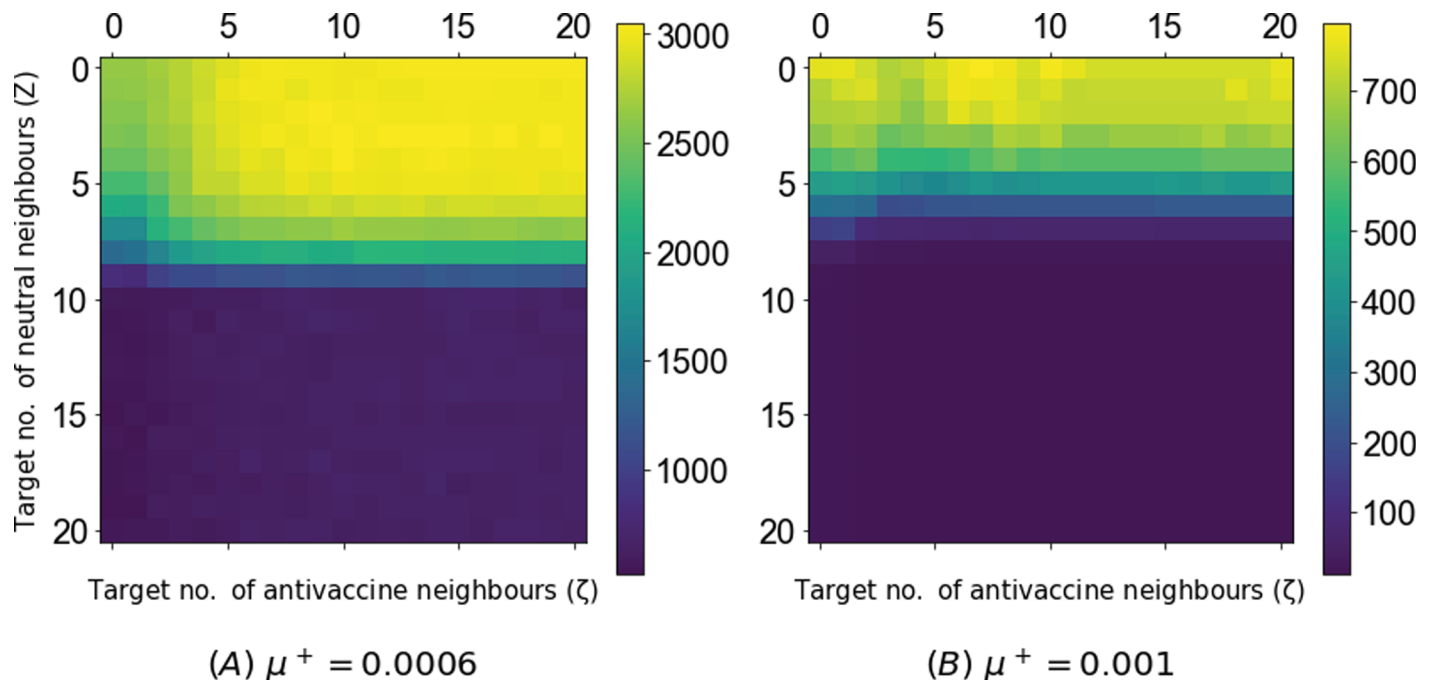


Fig 7. Average epidemic size using the DynAdvLocT dynamic campaign in the long-run setting of $\tau = \infty$. The figure shows the performance of the dynamic campaigns with $T = 50$ targets. The epidemic size is shown as a function of the target number of anti-vaccine neighbors ζ and the target number of neutral neighbors Z a neutral has at time t . The updating time is $t_r = 1$, and the social rate is $\omega = 0.006$ for both negative and positive $\omega^+ = \omega^-$. The general exposure influence rate for negative is $\mu^- = 0.001$ and the positive rate is shown in the figures captions.

<https://doi.org/10.1371/journal.pone.0318544.g007>

To elucidate the targeting strategy of this campaign, we illustrate in Fig 8 the neighborhood structure for the targeted agents of this campaign in conjunction with the evolution of opinion diffusion for both anti- and pro-vaccine adopters. In this campaign, by choosing a higher target number of neutral neighbors Z than the target number of anti-vaccine neighbors ζ , we prioritize the number of neutral neighbors over the number of anti-vaccine neighbors and vice versa. In the former scenario, this strategic shift directs positive allocation to agents more likely to propagate positive influence to a greater extent, as they have a larger number of neutral neighbors than anti-vaccine neighbors. This potentially will maximize the growth of pro-vaccine communities while restricting the growth of the anti-vaccine communities by being in proximity to them. In Fig 8A, an illustrative example of such a scenario is presented, with $Z = 8$ and $\zeta = 1$. As observed in the figure, this scenario focuses on targeting agents with the highest number of neutral neighbors and the smallest number of anti-vaccine neighbors. The corresponding evolution of opinions, depicted in Fig 8D and 8E, demonstrates that this targeting scheme maximizes the number of pro-vaccine adopters while simultaneously minimizing the number of anti-vaccine adopters, as indicated by the green lines. Consequently, it leads to a greater reduction in the epidemic size, as depicted in Fig 8F with the green bar.

Conversely, when the target number Z is smaller than ζ , we prioritize agents with a higher number of anti-vaccine neighbors than neutral neighbors. In this instance, we shift the targeting to focus on agents with a higher number of anti-vaccine neighbors and a relatively smaller number of neutral neighbors, see Fig 8B for an example with $Z = 1$ and $\zeta = 8$. Although emphasizing agents with more anti-vaccine neighbors can protect them from the anti-vaccine influence, it is less efficient in mitigating the overall propagation of this influence in the network. As depicted in Fig 8D and 8E, this targeting scheme results in a higher number of

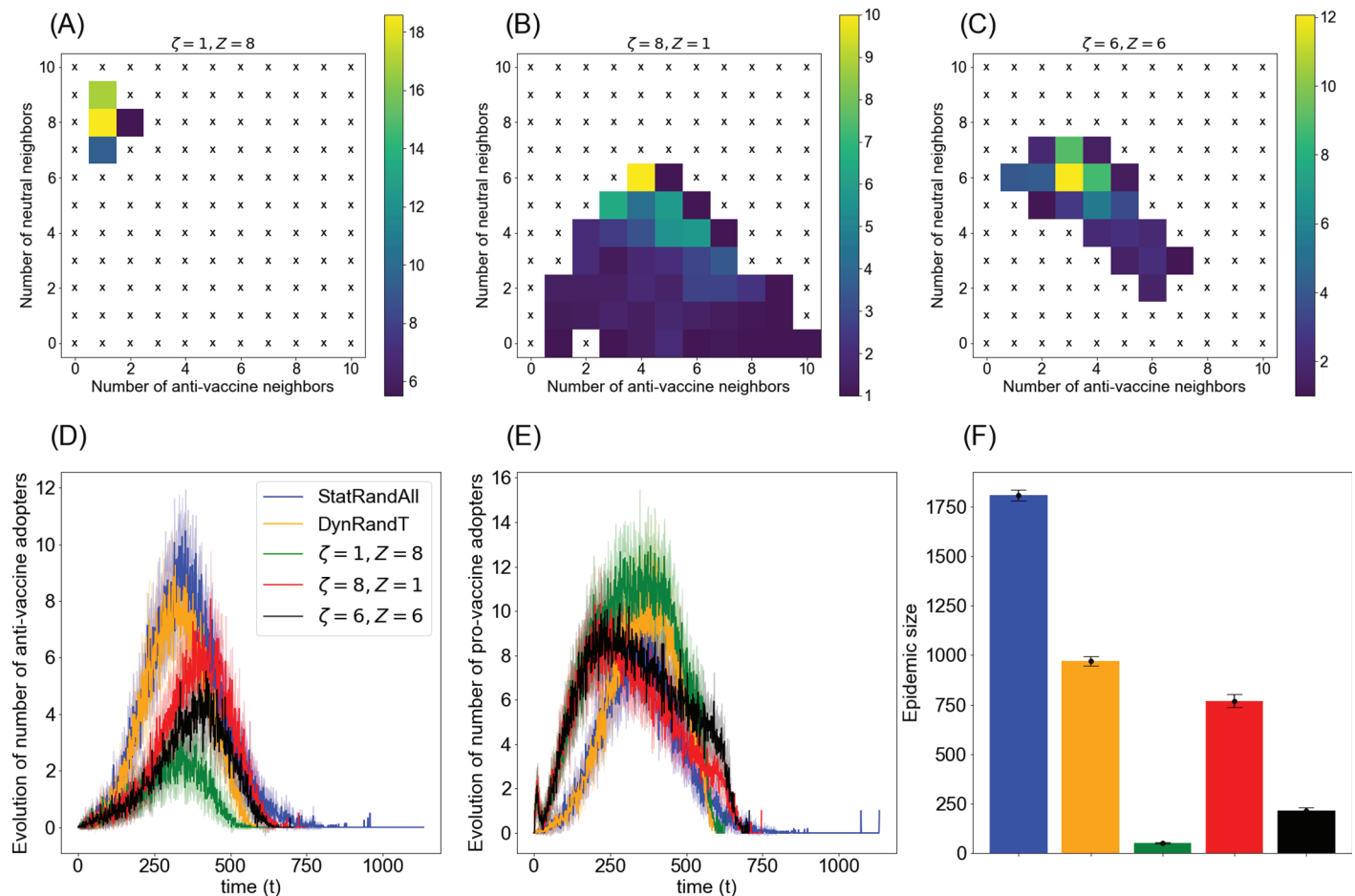


Fig 8. Targeting scheme for DynAdvLocT campaign. The top panels illustrate the neighborhood structure of the target set at a single time step $t=350$ during the opinion diffusion stage, specifically showing the number of anti-vaccine neighbors and pro-vaccine neighbors. These panels represent the average number of agents with x anti-vaccine neighbors and y neutral neighbors for various settings: (A) $\zeta = 1, Z = 8$, (B) $\zeta = 8, Z = 1$, (C) $\zeta = 6, Z = 6$. (D) and (E) illustrate the evolution of anti-vaccine opinion adopters and pro-vaccine opinion adopters, respectively, while panel (F) represents the corresponding epidemic size. 'x' indicates that no agent exists for that neighborhood pattern. The targeting analysis is an average of 15 simulations.

<https://doi.org/10.1371/journal.pone.0318544.g008>

anti-vaccine adopters and a lower number of pro-vaccine adopters compared to the first scenario (i.e., $Z = 1$ and $\zeta = 8$), as seen in the green and red lines. Correspondingly, it leads to a higher epidemic size, even though we are protecting the most vulnerable agents.

Moreover, in Fig 8C, we depict a scenario that assigns high priority to both Z and ζ , where $Z = \zeta = 6$. In this scenario, as observed, we target agents with a relatively high number of neutral neighbors and a high number of anti-vaccine neighbors, avoiding the smaller numbers of neutral neighbors targeted by the scenario $Z = 1, \zeta = 8$. Consequently, this approach proves more efficient than the scenario depicted in Fig 8B, resulting in lower numbers of anti-vaccine adopters, as depicted in the black line in Fig 8D, and accordingly, a smaller epidemic size in Fig 8F with the black bar. Despite this improvement over the previous scenario, the first scenario prioritizing neutral neighbors (Fig 8A) yields the best mitigation of negative influence and reduction in epidemic size. We further compare all three scenarios to random and dynamic random campaigns, depicted by the blue and orange colors, respectively, in opinion evolution and the corresponding epidemic size. As demonstrated in the figure, the DynAdvLocT scenario outperforms the benchmark cases in all scenarios.

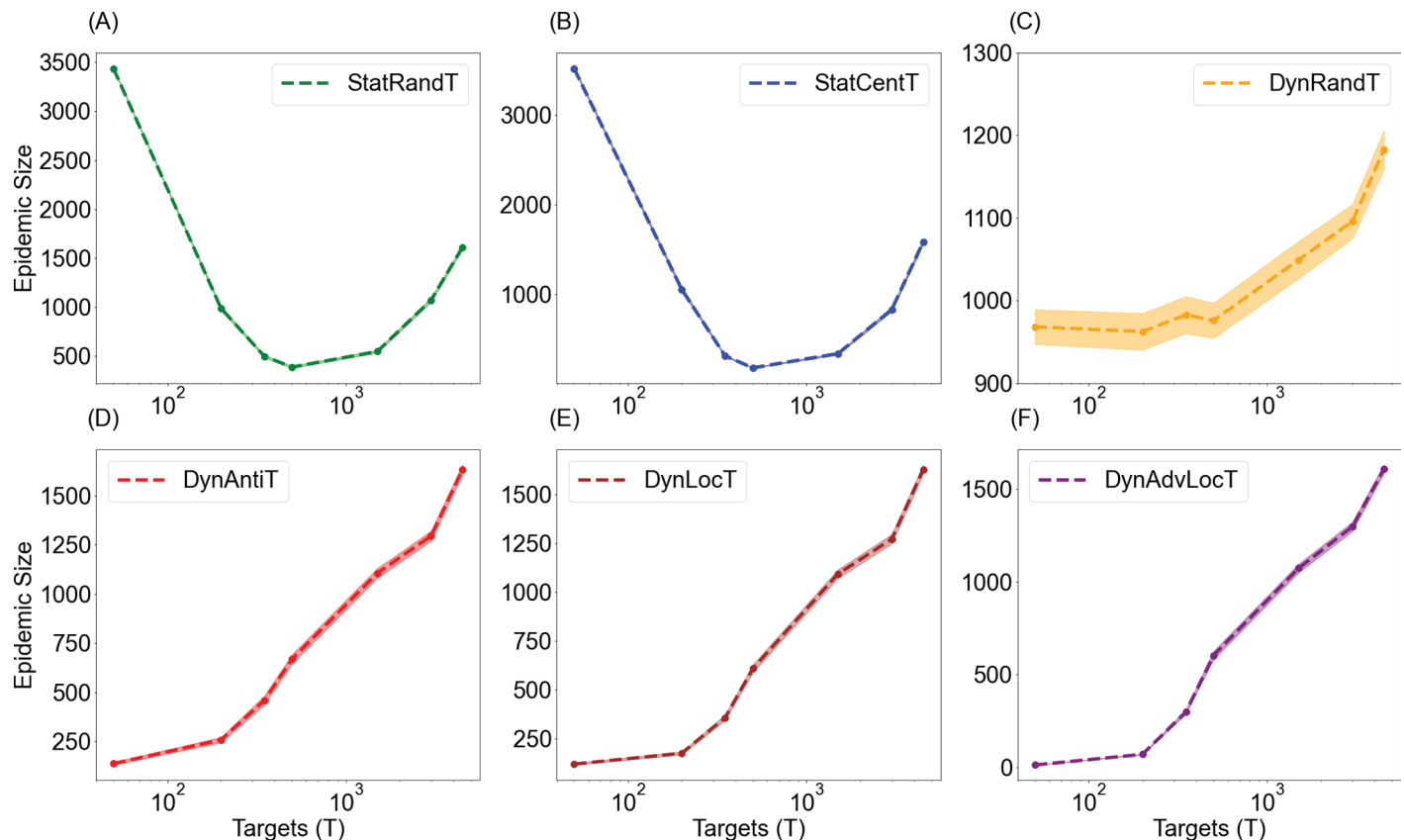


Fig 9. Epidemic size obtained with varying target sizes for targeted campaigns in the long-run setting where $\tau = \infty$. The figure illustrates the epidemic size obtained for all campaigns with general exposure rates $\mu^- = \mu^+ = 0.001$. The social rate is $\omega^+ = \omega^- = 0.006$ for all scenarios. For dynamic campaigns, the updating time interval is $t_r = 1$, for DynLocT $\zeta = 1$, and DynAdvLocT campaigns the target numbers of negative and neutral neighbours are $\zeta = 10, Z = 10$. For each scenario we generate 500 different networks, and perform 500 SIR model runs for each network.

<https://doi.org/10.1371/journal.pone.0318544.g009>

The impact of the target set size

The size of the target set is a crucial factor in determining the effectiveness of the targeted campaigns. Fig 9 demonstrates the correlation between the size of the target set and the extent of the epidemic in targeted campaigns. In the case of static campaigns, see Fig 9A and 9B, a larger target set results in better mitigation of anti-vaccine diffusion than a small target set. This is due to the positive allocation sticking around only these agents, and a relatively larger set ensuring a fair coverage in the network. However, we observed that a very large target set might act as noise and impede the focus of the campaign. For example, in the centrality-based campaign, after a certain point, i.e., $T=500$ which represents 10% of the population, the curve starts to increase again due to the inclusion of numerous low centrality agents in the target set, which hampers the centrality effects and introduces more randomness in the selection process.

In dynamic campaigns, on the other hand, the results have shown that smaller target group sizes, particularly in DynAntiT, DynLocT, and DynAdvLocT, yield better reduction compared to larger sizes, as depicted in Fig 9(D)–9(F). The dynamic random campaign demonstrates a slight increase as the target size increases. This suggests that it is more effective to direct resources to a smaller yet changeable target set. This observation can be attributed

to the fact that a smaller size allows for more selective targeting of individuals who meet the campaign's criteria and are more likely to be influenced. On the contrary, a larger target set may include individuals who are less susceptible to the negative influence, introducing more randomness in the selection process and resulting in decreased effectiveness. Furthermore, the positive strength allocated to a campaign is typically distributed evenly across the target group. As a result, a change in the target size can lead to a change in the strength allocated per individual.

Cross-campaign comparison

In this section, we present a comparison of the proposed campaigns to evaluate their performance in reducing the epidemic size. Further performance evaluation of the campaigns' impact on disease dynamics during the course of the epidemic can be seen in Fig 2 in S1 Appendix. As we see in Fig 2 in the S1 Appendix, our campaign achieves a reduction in peak numbers of infections proportionate to the sizes of the outbreaks. In Fig 10, we compare the best scenarios for each campaign, depicting three distinct states of strength allocation in the general exposure for negative and positive campaigns, considering a high social rate—a crucial scenario in which anti-vaccine communities can expand significantly. The aim is to investigate which campaign can mitigate this expansion most effectively. The figure also demonstrates the long-run behavior of the system. Across all scenarios, advanced local information campaigns, particularly DynAdvLocT, achieve the best performance in reducing the epidemic size.

In situations where the positive general exposure rate is much smaller than the negative general exposure rate (i.e., $\mu^+ \ll \mu^-$), the best practice is to use DynAdvLocT with slower updates (i.e., $t_r = 20$) if we assume complete knowledge of the population's vaccine-related

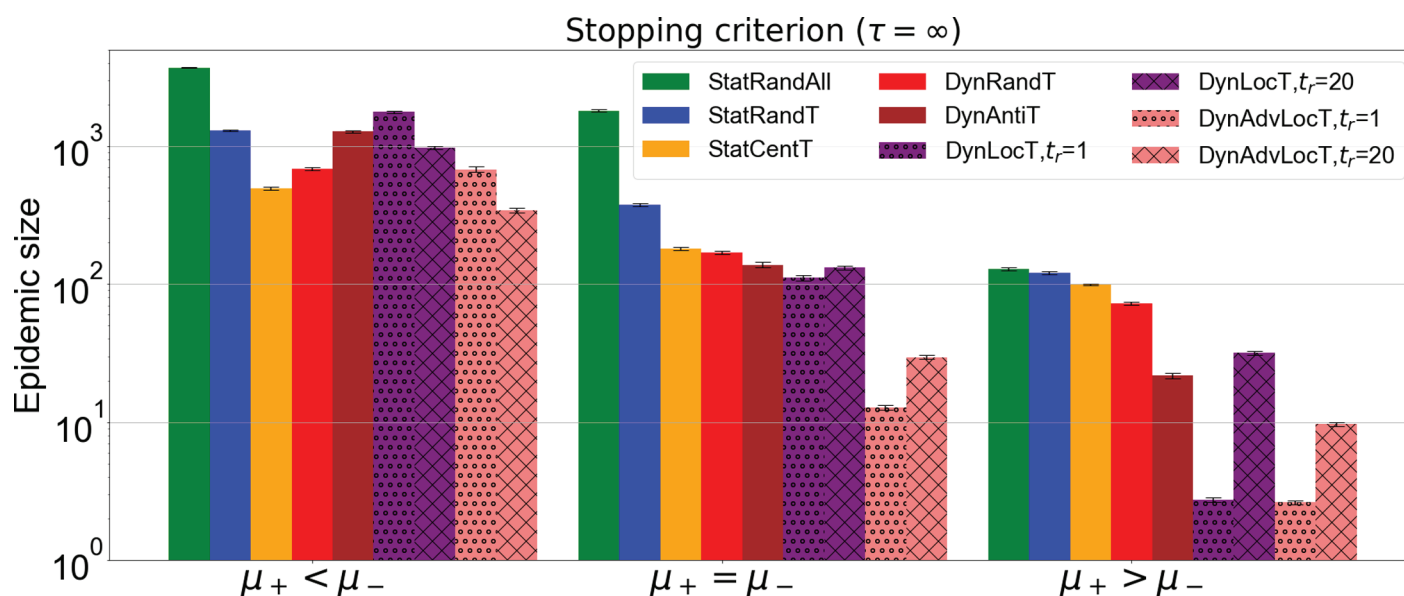


Fig 10. Cross-campaign epidemic size comparison with $\tau = \infty$. The figure illustrates the epidemic size obtained for all campaigns with different positive rates μ^+ compared to negative rate μ^- . For all campaigns, $\mu^- = 0.001$. First group: $\mu^+ = 0.0006$, second group: $\mu^+ = 0.001$, and third group: $\mu^+ = 0.002$. Social rate is $\omega = 0.006$ for all scenarios. Target set size $T = 500$ for static campaigns, i.e., StatRandT, and StatCentT, and $T = 50$ for the other dynamic campaigns. For dynamic campaigns, the updating time is $t_r = 20$, in addition we include $t_r = 1$ for DynLocT and DynAdvLocT campaigns. In addition, for DynLocT $\zeta = 1$, for DynAdvLocT $\zeta = Z = 10$.

<https://doi.org/10.1371/journal.pone.0318544.g010>

attitudes. The next best option is the centrality-based campaign when we have incomplete knowledge about vaccine attitudes. The former results in an epidemic size of 345 ± 13 , while the latter results in 493 ± 15 .

When both negative and positive general exposures exert the same rate of influence (i.e., $\mu^+ = \mu^-$), DynAdvLocT with fast updates (i.e., $t_r = 1$) is the most effective, while centrality-based and other dynamic campaigns produce relatively similar performance. Finally, when the positive general exposure rate is higher than the negative one (i.e., $\mu^+ > \mu^-$), the best practice is to use either DynLocT or DynAdvLocT with fast updates (i.e., $t_r = 1$).

From Fig 10, it is observed that although the random strategy StatRandAll shown by green bars reduced the epidemic size, it is not the most efficient strategy compared to other campaigns, as the resulting epidemic size is higher than that of the others. The static random campaign StatRandT shown by blue bars follows a similar pattern but performs better than the random campaign. This observation, as investigated earlier, is due to the fact that the random campaign StatRandAll fails to exert more influence over time, and opinions become socially-driven. In contrast, the targeted random campaign StatRandT targets fixed positions in the network, creating barriers that prevent the clustering of anti-vaccine communities, making it slightly more effective than the random campaign StatRandAll. This observation is consistent with the study conducted by [42], where the authors demonstrated that a random selection of the seed set resulted in poor mitigation of misinformation propagation.

In Fig 11, we consider a scenario where negative information spreads faster than positive information, i.e., $\omega^- > \omega^+$. This is motivated by existing literature, which highlights distinct diffusion dynamics between positive and negative information, with negative information spreading more rapidly and extensively than positive information [67]. This raises critical questions: Can the diffusion of negative information still be effectively controlled in such a context? Moreover, how do the proposed campaigns perform under these conditions?

As shown in Fig 11, although the performance is slightly worse compared to the scenario with faster positive spreading depicted in Fig 10, it is still possible to effectively contain the diffusion and maintain a low epidemic size, particularly with the use of the DynAdvLocT strategy. Furthermore, we also note that the performance improves significantly as the positive budget increases.

Discussion

In this paper, we have investigated the impact of different strategic positive campaigns for spreading positive vaccine-related information to combat the spread of negative vaccine-related information. We also examined how these campaigns affect the diffusion of anti-vaccine opinions and the connectivity between emerging anti-vaccine communities, thereby leading to a reduction in the epidemic size. We demonstrated that the existence of positive influence propagation has a positive impact on mitigating the flow of negative influence, leading to improved vaccination coverage and, as a result, reduces the epidemic size. However, this impact varies across different campaigning approaches.

One crucial factor in the diffusion of anti-vaccine sentiments within a social network is the level of social influence between individuals; as the social contagion rate increases, the size of the anti-vaccine communities grows, consequently increasing the epidemic size. This phenomenon can be observed in Fig 3, specifically within the benchmark case where the scenario involves only anti-vaccine diffusion (depicted by the green line), and it persists despite the concurrent presence of pro-vaccine propagation through a random campaign. These results are consistent with previous studies that investigated a similar problem and demonstrated the

role of social interactions in promoting the growth of anti-vaccine communities, thus increasing the epidemic size [11,22]. We then demonstrated that targeted campaigns can effectively contain the spread of anti-vaccine diffusion in such a scenario (see Fig 4).

In this study, we demonstrated that a targeted campaign based on the network structure, specifically aimed at individuals with high centrality, proves effective in reducing the spread of negative opinions and mitigating social contagion. This approach places positive seeds strategically on the most central bridges within the network, thus preventing the merging of anti-vaccine communities more efficiently. However, this method requires a large number of targets to be efficient, making it impractical in limited-resource settings, see Fig 9B.

As demonstrated above selecting targets based on local negative information proves to be the most effective strategy. By focusing on individuals who are more vulnerable to negative influences, this technique outperforms random selection and even outperforms the centralized approach. It also demonstrates efficacy even with a small target set. Quantifying the amount of negative influence on neutral social contacts yields further reductions in the size of the epidemic. Moreover, incorporating the potential for maximizing positive influence, by considering the number of neutrals for each candidate, leads to higher effectiveness, as seen in DynAdvLocT strategy. However, it is important to note that these local information-based campaigns assume complete knowledge of the vaccine-related attitudes within the population.

Moving beyond the exploration of effective targeting strategies, several historical instances exemplify the detrimental effects of vaccine misinformation, where negative beliefs have profoundly impeded public health efforts. The spread of misinformation during the COVID-19 pandemic resulted in increased vaccine hesitancy and low vaccination rate [68]. Similarly,

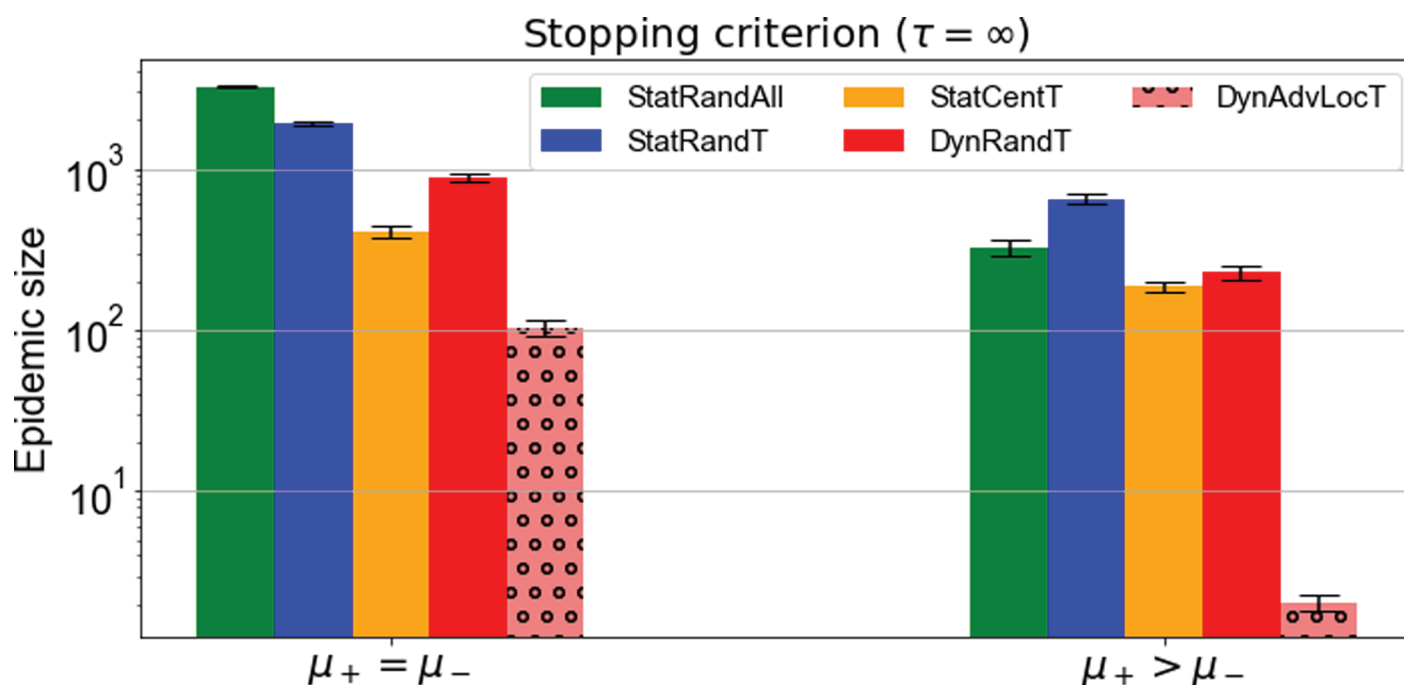


Fig 11. Cross-campaign epidemic size comparison with $\tau = \infty$. The figure illustrates the epidemic size obtained for the best campaigns with different positive rates μ^+ compared to negative rate μ^- and for lower positive social rate. For all campaigns, $\mu^- = 0.001$. First group: $\mu_+ = 0.001$ and second group: $\mu_+ = 0.002$. Social rate is $\omega^- = 0.006$, $\omega^+ = 0.003$ for all scenarios. Target set size $T = 500$ for static campaigns, i.e., StatRandT, and StatCentT, and $T = 50$ for the other dynamic campaigns. For dynamic campaigns, the updating time is $t_r = 20$ for DynRandT and $t_r = 1$ for DynAdvLocT. For DynAdvLocT $\zeta = Z = 10$. The results are the average of 50 simulations.

<https://doi.org/10.1371/journal.pone.0318544.g011>

during the Ebola outbreak in North Kivu, a notable association was observed between the mistrust in health systems and the belief in misinformation, which led to reduced inclination in adopting preventive behaviors, including acceptance of Ebola vaccines [69]. Additionally, the year 2019, witnessed a resurgence of measles due to a significant decline in vaccine coverage, resulting from the spread of anti-vaccine attitudes as a significant cause [53]. Such cases exemplify the pivotal role of accurate information in managing and mitigating the effects of misinformation associated with various infectious diseases.

Locally tailored approaches to improving health promotion are vital. Our approaches here need further development, but the modelling is designed to be flexible to support local needs and thus can incorporate localised scenarios with regard to the rate of dissemination of good and bad public health information, and the number of positive, neutral and negative nodes. It can also be adapted to mimic online or offline dissemination. In addition, the current model operates on the assumption of comprehensive knowledge regarding vaccine-related attitudes within the social network. Full knowledge of the attitude of every individual is not realistic in practice; however, obtaining some information is feasible from processes such as social network analysis of data from social media platforms. For instance, empirical studies leveraging data from online social networks have applied sentiment analysis and machine learning algorithms to categorize individuals' attitudes into distinct states such as pro-vaccine, anti-vaccine, and neutral towards vaccination [28,70–72]. Additionally, public attitudes toward vaccines have been explored through the analysis of real-time, spatial-temporal, and socio-demographic data from social media, unveiling the spatial distribution of these attitudes [34,73,74]. Such platforms and techniques facilitate real-time, socio-geographic monitoring of public attitudes, aiding health campaigns in implementing optimal interventions.

The effectiveness of many real-world interventions in addressing vaccine hesitancy and improving vaccination uptake has been demonstrated through a variety of real-world campaigns. For example, a social media campaign promoting COVID-19 vaccination in Nigeria showed a positive effect of the campaign in the targeted states compared to other states, with higher pro-vaccination norms strongly associated with increased vaccination rates [75]. Similarly, a recent study [76] examines the effectiveness of a culturally tailored outreach campaign aimed at improving COVID-19 vaccine uptake among African immigrants in Philadelphia. The study found that community-based programs effectively addressed barriers such as mistrust and misinformation, leading to increased vaccine uptake and reduced hesitancy. Moreover, a systematic review of various parental intervention campaigns aimed at childhood immunization, presented in [77], found that reminder-based and education-based interventions significantly enhance children's vaccination uptake. Another study investigates the 'PromoVac' strategy which uses motivational interviews method [78], conducted during post-partum hospitalization to target mothers and encourage infant immunization. The findings revealed that this intervention significantly improved vaccination rates at key milestones (3, 5, 7, 13, 19, and 24 months) and increased the likelihood of complete vaccination coverage throughout infancy.

Although the model provides valuable insights, several inherent limitations should be acknowledged to fully understand its scope and applicability. First, the presented results are limited to the assumption of committed agents who do not change their opinions. However, the proposed heuristics could be extended to a broader range of opinion diffusion models and integrated into models that allow opinions to switch back and forth, such as the voter model and epidemic models like the SIS model. Additionally, opinions in our model are not influenced by disease spread, as we address the diffusion processes of information and disease separately (in line with similar studies, e.g., [8]). Information spread is assumed to occur before

the onset of disease, aligning with patterns typically observed in vaccine-preventable childhood diseases. An additional limitation of this study is the use of a single network to represent both information and disease diffusion, modeled as a physical or face-to-face network structure. Future research would benefit from exploring the implications of employing distinct network structures tailored to each diffusion process in a multi-layer settings (e.g., [18,46]). Another limitation of the model is the resolution of the available local information on individuals' vaccine attitudes, as assessing these attitudes with complete accuracy can be challenging. Consequently, further investigation is required to improve our understanding of campaign resilience to gaps in knowledge. Similarly, the proposed heuristics, particularly those based on information, though efficient, are relatively simple and can potentially be further improved.

Conclusion

The purpose of this study is to investigate effective mechanisms to mitigate the spread of anti-vaccine attitudes and reduce the size of epidemics by applying positive counter-campaigns that spread positive vaccine-related sentiments. We proposed efficient heuristics to combat negative influence propagation. We have demonstrated that these campaigns can impede the flow of anti-vaccine attitudes and changed the distribution of unvaccinated individuals within the population, which in turn changed the structures of anti-vaccine communities and suppressed the spread of epidemics. Our study has proposed strategies based on two main paradigms: social network structure and negative local information, in addition to two control schemes static and dynamic. Through extensive experiments, we systematically studied and analyzed the performance of the proposed strategies in reducing the size of epidemic, identifying their strengths and limitations.

We have demonstrated that targeted campaigns that select a subset of the population based on certain criteria have been found to be more effective in suppressing the epidemic compared to random campaign, particularly in scenarios with high levels of social interactions. The latter approach results in poor mitigation compared to other methods. In contrast, centrality-based and local information-based strategies have shown superior performance. The centrality-based campaign targets central nodes which effectively hinder the merging of emerging communities, while the local information-based methods prevent the most vulnerable agents from being negatively influenced. Moreover, the dynamic control approach, which involves continuous updating of the target set, has been found to be more effective in suppressing the epidemic compared to a static control approach. This approach provides continuous and iterative exposure to positive messaging while keeping the campaign involved with the evolution of anti-vaccine attitudes. Furthermore, prioritizing those susceptible based on their neighborhood state performs even better in mitigating negative influence propagation.

Supporting information

S1 Appendix. Supporting information file with additional analysis.

(PDF)

S1 Data. Data files with detailed results.

(RAR)

Acknowledgments

The authors acknowledge the use of the IRIDIS High Performance Computing Facility in the completion of this work.

Author contributions

Conceptualization: Sarah Alahmadi, Rebecca Hoyle, Michael Head, Markus Brede.

Formal analysis: Sarah Alahmadi.

Investigation: Sarah Alahmadi, Rebecca Hoyle, Michael Head, Markus Brede.

Methodology: Sarah Alahmadi, Rebecca Hoyle, Michael Head, Markus Brede.

Software: Sarah Alahmadi.

Supervision: Rebecca Hoyle, Michael Head, Markus Brede.

Validation: Sarah Alahmadi, Rebecca Hoyle, Michael Head, Markus Brede.

Visualization: Sarah Alahmadi.

Writing – original draft: Sarah Alahmadi.

Writing – review & editing: Sarah Alahmadi, Rebecca Hoyle, Michael Head, Markus Brede.

References

1. WHO. Ten health issues who will tackle this year. (2019). Available from: <https://www.who.int/news-room/spotlight/ten-threats-to-global-health-in-2019>
2. Dubé E, Laberge C, Guay M, Bramadat P, Roy R, Bettinger JA. Vaccine hesitancy: an overview. *Hum Vaccin Immunotherap*. 2013;9:1763–73. <https://doi.org/10.4161/hv.24657>
3. Zhang H, Shu P, Wang Z, Tang M, Small M. Preferential imitation can invalidate targeted subsidy policies on seasonal-influenza diseases. *Appl Math Comput*. 2017;294:332–42. <https://doi.org/10.1016/j.amc.2016.08.057>
4. Zhang H, Wu Z, Tang M, Lai Y. Effects of behavioral response and vaccination policy on epidemic spreading—an approach based on evolutionary-game dynamics. *Sci Rep*. 2014;4(1):1–10. <https://doi.org/10.1038/srep05666>
5. Ichinose G, Kurisaku T. Positive and negative effects of social impact on evolutionary vaccination game in networks. *Phys A: Statist Mech Appl*. 2017;468:84–90. <https://doi.org/10.1016/j.physa.2016.10.017>
6. Wang X, Jia D, Gao S, Xia C, Li X, Wang Z. Vaccination behavior by coupling the epidemic spreading with the human decision under the game theory. *Appl Math Comput*. 2020;380:125232. <https://doi.org/10.1016/j.amc.2020.125232>
7. Zhang H, Zhang J, Zhou C, Small M, Wang B. Hub nodes inhibit the outbreak of epidemic under voluntary vaccination. *New J Phys*. 2010;12(2):023015. <https://doi.org/10.1088/1367-2630/12/2/023015>
8. Salathe M, Bonhoeffer S. The effect of opinion clustering on disease outbreaks. *J Roy Soc Interface*. 2008;5:1505–8. <https://doi.org/10.1098/rsif.2008.0271>
9. Funk S, Gilad E, Watkins C, Jansen VA. The spread of awareness and its impact on epidemic outbreaks. *Proc Natl Acad Sci U S A*. 2009;106(16):6872–7. <https://doi.org/10.1073/pnas.0810762106> PMID: 19332788
10. Ruan Z, Tang M, Liu Z. Epidemic spreading with information-driven vaccination. *Phys Rev. E Statist Nonl Soft Matter Phys*. 2012;86(3 Pt 2):036117. <https://doi.org/10.1103/PhysRevE.86.036117> PMID: 23030990
11. Campbell E, Salathé Marcel., Salathe M. Complex social contagion makes networks more vulnerable to disease outbreaks. *Sci Rep*. 2013;3(1):1–6. <https://doi.org/10.1038/srep01905>
12. da Silva PCV, Velasquez-Rojas F, Connaughton C, Vazquez F, Moreno Y, Rodrigues FA. Epidemic spreading with awareness and different timescales in multiplex networks. *Phys Rev E*. 2019;100:032313. <https://doi.org/10.1103/PhysRevE.100.032313>
13. Mehta RS, Rosenberg NA. Modelling anti-vaccine sentiment as a cultural pathogen. *Evolution Hum Sci*. 2020;2:e21. <https://doi.org/10.1017/ehs.2020.17> PMID: 37588376
14. Fu F, Rosenbloom DI, Wang L, Nowak MA. Imitation dynamics of vaccination behaviour on social networks. *Proc Biol Sci*. 2011;278(1702):42–9. <https://doi.org/10.1098/rspb.2010.1107> PMID: 20667876

15. Cardillo A, Reyes-Suarez C, Naranjo F, Gomez-Gardenes J. Evolutionary vaccination dilemma in complex networks. *Phys Rev E*. 2013;88:032803. <https://doi.org/10.1103/PhysRevE.88.032803>
16. Kabir K, Kuga K, Tanimoto J. Effect of information spreading to suppress the disease contagion on the epidemic vaccination game. *Chaos Solitons Fract*. 2019;119:180–7. <https://doi.org/10.1016/j.chaos.2018.12.023>
17. Kabir K, Tanimoto J. Vaccination strategies in a two-layer SIR/V–UA epidemic model with costly information and buzz effect. *Commun Nonl Sci Numer Simulat*. 2019;76:92–108. <https://doi.org/10.1016/j.cnsns.2019.04.007>
18. Yin Q, Wang Z, Xia C, Bauch CT. Impact of co-evolution of negative vaccine-related information, vaccination behavior and epidemic spreading in multilayer networks. *Commun Nonl Sci Numer Simulat*. 2022;109:106312. <https://doi.org/10.1016/j.cnsns.2022.106312>
19. Dube E, Vivion M, MacDonald NE. Vaccine hesitancy, vaccine refusal and the anti-vaccine movement: influence, impact and implications. *Exp Rev Vaccines*. 2015;14:99–117. <https://doi.org/10.1586/14760584.2015.964212>
20. Farooq F, Rathore F. COVID-19 vaccination and the challenge of infodemic and disinformation. *J Korean Med Sci*. 2021;36(10):e78. <https://doi.org/10.3346/jkms.2021.36.e78>
21. Sontag A, Rogers T, Yates CA. Misinformation can prevent the suppression of epidemics. *J Roy Soc Interface*. 2022;19(188):20210668. <https://doi.org/10.1098/rsif.2021.0668> PMID: 35350880
22. Dorso CO, Medus A, Balenzuela P. Vaccination and public trust: A model for the dissemination of vaccination behaviour with external intervention. *Phys A: Statist Mech Appl*. 2017;482:433–43. <https://doi.org/10.1016/j.physa.2017.04.112>
23. Dai X, Zhu P, Guo Y, Wang Z. Coevolution of vaccination opinions and awareness affecting the spread of epidemics. *IEEE Access*. 2019;7:61558–69. <https://doi.org/10.1109/access.2019.2902856>
24. Mumtaz N, Green C, Duggan J. Exploring the effect of misinformation on infectious disease transmission. *systems*. 2022;10;50. <https://doi.org/10.3390/systems10020050>
25. Chen J, Liu Y, Yue J, Duan X, Tang M. Coevolving spreading dynamics of negative information and epidemic on multiplex networks. *Nonl Dynam*. 2022;110;4;3881–91. <https://doi.org/10.1007/s11071-022-07776-x>
26. Centola D. The spread of behavior in an online social network experiment. *Science*. 2010;329(5996):1194–7. <https://doi.org/10.1126/science.1185231> PMID: 20813952
27. Romero DM, Meeder B, Kleinberg J. Differences in the mechanics of information diffusion across topics: idioms, political hashtags, and complex contagion on twitter. *Proceedings of the 20th International Conference on World Wide Web—WWW 2011*. New York, NY, USA: ACM Press; 2011. p. 695–704. <https://doi.org/10.1145/1963405.1963503>
28. Salathe M, Khandelwal S. Assessing vaccination sentiments with online social media: implications for infectious disease dynamics and control. *PLoS Comput Biol*. 2011;7(10):e1002199. <https://doi.org/10.1371/journal.pcbi.1002199>
29. Omer SB, Salmon DA, Orenstein WA, Dehart MP, Halsey N. Vaccine refusal, mandatory immunization, and the risks of vaccine-preventable diseases. *New Engl J Med*. 2009; 360(19):1981–8. <https://doi.org/10.1056/NEJMsa0806477> PMID: 19420367
30. Yuan X, Schuchard RJ, Crooks AT. Examining emergent communities and social bots within the polarized online vaccination debate in Twitter. *Soc Media Soc*. 2019;5(3):2056305119865465. <https://doi.org/10.1177/2056305119865465>
31. Lieu TA, Ray GT, Klein NP, Chung C, Kulldorff M. Geographic clusters in underimmunization and vaccine refusal. *Pediatrics*. 2015;135(2):280–9. <https://doi.org/10.1542/peds.2014-2715> PMID: 25601971
32. Gromis A, Liu K. Spatial clustering of vaccine exemptions on the risk of a measles outbreak. *Pediatrics*. 2022;149(1):e2021050971. <https://doi.org/10.1542/peds.2021-050971> PMID: 34866158
33. Bello-Ortiz G, Hernandez-Castro J, Camacho D. Detecting discussion communities on vaccination in Twitter. *Future Gen Comput Syst*. 2017;66:125–36. <https://doi.org/10.1016/j.future.2016.06.032>
34. Cheng T, Han B, Liu Y. Exploring public sentiment and vaccination uptake of COVID-19 vaccines in England: a spatiotemporal and sociodemographic analysis of Twitter data. *Front Publ Health*. 2023;11. <https://doi.org/10.3389/fpubh.2023.1193750>
35. Pham DV, Nguyen GL, Nguyen TN, Pham CV, Nguyen AV. Multi-topic misinformation blocking with budget constraint on online social networks. *IEEE Access*. 2020;8:78879–89. <https://doi.org/10.1109/access.2020.2989140>
36. Zareie A, Sakellariou R. Rumour spread minimization in social networks: a source-ignorant approach. *Online Soc Netw Media*. 2022;29:100206. <https://doi.org/10.1016/j.osnem.2022.100206>

37. Budak C, Agrawal D, El Abbadi A. Limiting the spread of misinformation in social networks. In: Proceedings of the 20th International Conference on World Wide Web. 2011. p. 665–74. <https://doi.org/10.1145/1963405.1963499>
38. Liu W, Yue K, Wu H, Li J, Liu D, Tang D. Containment of competitive influence spread in social networks. *Knowl-Based Syst.* 2016;109:266–75. <https://doi.org/10.1016/j.knosys.2016.07.008>
39. Tong A, Du D, Wu W. On misinformation containment in online social networks. *Adv Neural Inf Process Syst.* 2018;31.
40. Yang L, Li Z, Giua A. Rumor containment by spreading correct information in social networks. In: 2019 American Control Conference (ACC). 2019. p. 5608–13. <https://doi.org/10.23919/ACC.2019.8814884>
41. Yang L, Li Z, Giua A. Containment of rumor spread in complex social networks. *Inf Sci.* 2020;506:113–30. <https://doi.org/10.1016/j.ins.2019.07.055>
42. Zhang H, Zhang H, Li X, Thai MT. Limiting the spread of misinformation while effectively raising awareness in social networks. In: Computational Social Networks: 4th International Conference, CSoNet 2015, Beijing, China, 2015 August 4–6, Proceedings 4. Springer; 2015. p. 35–47. https://doi.org/10.1007/978-3-319-21786-4_4
43. Adeyanju GC, Engel E, Koch L, Ranzinger T, Shahid IBM, Head MG, et al. Determinants of influenza vaccine hesitancy among pregnant women in Europe: a systematic review. *Eur J Med Res.* 2021;26(1):1–12. <https://doi.org/10.1186/s40001-021-00584-w>
44. Marzo RR, Ahmad A, Islam MS, Essar MY, Heidler P, King I, et al. Perceived COVID-19 vaccine effectiveness, acceptance, and drivers of vaccination decision-making among the general adult population: a global survey of 20 countries. *PLoS Neglect Trop Dis.* 2022;16(1):e0010103. <https://doi.org/10.1371/journal.pntd.0010103> PMID: 35089917
45. Yin Q, Wang Z, Xia C. Information-epidemic co-evolution propagation under policy intervention in multiplex networks. *Nonl Dynam.* 2023;111(15):14583–95. <https://doi.org/10.1007/s11071-023-08581-w>
46. Fügenschuh M, Fu F. Overcoming vaccine hesitancy by multiplex social network targeting: an analysis of targeting algorithms and implications. *Appl Netw Sci.* 2023;8:67. <https://doi.org/10.1007/s41109-023-00595-y>
47. Ancona, C., Iudice, F., Garofalo, F. De Lellis, P. A model-based opinion dynamics approach to tackle vaccine hesitancy. *Sci Rep.* 2022;12:11835. <https://doi.org/10.1038/s41598-022-15082-0>
48. Romero Moreno G, Chakraborty S, Brede, M. Shadowing and shielding: effective heuristics for continuous influence maximisation in the voting dynamics. *Plos One.* 2021;16(6):e0252515. <https://doi.org/10.1371/journal.pone.0252515>
49. Romero Moreno G, Tran-Thanh L, Brede M. Continuous influence maximisation for the voter dynamics: is targeting high-degree nodes a good strategy? In: Proceedings of the 19th International Conference on Autonomous Agents and MultiAgent Systems. 2020. p. 1981–3
50. Prieto Curiel R, González Ramírez H. Vaccination strategies against COVID-19 and the diffusion of anti-vaccination views. *Sci Rep.* 2021;11(1):6626. <https://doi.org/10.1038/s41598-021-85555-1> PMID: 33758218
51. Wijayanto AW, Murata T. Effective and scalable methods for graph protection strategies against epidemics on dynamic networks. *Appl Netw Sci.* 2019;4:1–18. <https://doi.org/10.1007/s41109-019-0122-7>
52. Shi Q, Wang C, Ye D, Chen J, Feng Y, Chen C. Adaptive influence blocking: minimizing the negative spread by observation-based policies. In: 2019 IEEE 35th International Conference on Data Engineering (ICDE). 2019. p. 1502–13. <https://doi.org/10.1109/ICDE.2019.00135>
53. Hotez P, Nuzhath T, Colwell B. Combating vaccine hesitancy and other 21st century social determinants in the global fight against measles. *Curr Opin Virol.* 2020;41:1–7. <https://doi.org/10.1016/j.coviro.2020.01.001>
54. Tatsukawa Y, Arefin MR, Tanaka M, Tanimoto J. Free ticket, discount ticket or intermediate of the best of two worlds—Which subsidy policy is socially optimal to suppress the disease spreading? *J Theor Biol.* 2021;520:110682. <https://doi.org/10.1016/j.jtbi.2021.110682> PMID: 33744309
55. Kermack WO, McKendrick AG. A contribution to the mathematical theory of epidemics. *Proc Roy Soc Lond. Ser A: Contain Papers Math Phys Charact.* 1927;115:700–21. <https://doi.org/10.1098/rspa.1927.0118>
56. Watts DJ, Strogatz SH. Collective dynamics of ‘small-world’ networks. *Nature.* 1998;393(6684):440–2. <https://doi.org/10.1038/30918> PMID: 9623998
57. Barrat A, Weigt M. On the properties of small-world network models. *Eur Phys J B* 2000;13(3):547–60. <https://doi.org/10.1007/s100510050067>
58. Latora V, Marchiori M. Efficient behavior of small-world networks. *Phys Rev Lett.* 2001;87(19):198701. <https://doi.org/10.1103/PhysRevLett.87.198701> PMID: 11690461

59. Schmidt A, Zollo F, Scala A, Betsch C, Quattrociocchi W. Polarization of the vaccination debate on Facebook. *Vaccine*. 2018;36(25):3606–12. <https://doi.org/10.1016/j.vaccine.2018.05.040>
60. Mønsted B, Lehmann, S. Characterizing polarization in online vaccine discourse—a large-scale study. *PloS One*. 2022;17(2):e0263746. <https://doi.org/10.1371/journal.pone.0263746> PMID: 35139121
61. House T, Ross JV, Sirl D. How big is an outbreak likely to be? Methods for epidemic final-size calculation. *Proc Roy Soc A: Math Phys Eng Sci*. 2013;469(2150):20120436. <https://doi.org/10.1098/rspa.2012.0436>
62. Konstantinou P, Georgiou K, Kumar N, Kyprianidou M, Nicolaidis C, Karekla M, et al. Transmission of vaccination attitudes and uptake based on social contagion theory: a scoping review. *Vaccines*. 2021;9(6):607. <https://doi.org/10.3390/vaccines9060607> PMID: 34198885
63. Brandes U. A faster algorithm for betweenness centrality. *J Math Sociol*. 2001;25:163–77. <https://doi.org/10.1080/0022250X.2001.9990249>
64. Latora V, Nicosia V, Russo G. Centrality measures. In: *Complex networks: principles, methods and applications*. Cambridge: Cambridge University Press; 2017. p. 31–68. <https://doi.org/10.1017/9781316216002.004>
65. Zhang J, Luo Y. Degree centrality, betweenness centrality, and closeness centrality in social network. In: *Proceedings of the 2017 2nd International Conference on Modelling, Simulation and Applied Mathematics (MSAM2017)*. Atlantis Press; 2017. p. 300–3. <https://doi.org/10.2991/msam-17.2017.68>
66. Lynch S, Tran-Thanh L, Santos F, et al. Fostering cooperation in structured populations through local and global interference strategies. In: *27th International Joint Conference on Artificial Intelligence and the 23rd European Conference on Artificial Intelligence*. 2018. p. 289–95. <https://doi.org/10.24963/ijcai.2018/40>
67. Tsugawa S, Ohsaki H. Negative messages spread rapidly and widely on social media. In: *Proceedings of the 2015 ACM on Conference on Online Social Networks*. 2015. p. 151–60. <https://doi.org/10.1145/2817946.2817962>
68. Lee SK, Sun J, Jang S, Connelly S. Misinformation of COVID-19 vaccines and vaccine hesitancy. *Sci Rep*. 2022;12(1):13681. <https://doi.org/10.1038/s41598-022-17430-6> PMID: 35953500
69. Vinck P, Pham PN, Bindu KK, Bedford J, Nilles EJ. Institutional trust and misinformation in the response to the 2018–19 Ebola outbreak in North Kivu, DR Congo: a population-based survey. *Lancet Infect Dis*. 2019;19(5):529–36. [https://doi.org/10.1016/S1473-3099\(19\)30063-5](https://doi.org/10.1016/S1473-3099(19)30063-5) PMID: 30928435
70. D'Andrea E, Ducange P, Bechini A, Renda A, Marcelloni F. Monitoring the public opinion about the vaccination topic from tweets analysis. *Exp Syst Appl*. 2019;116:209–26. <https://doi.org/10.1016/j.eswa.2018.09.009>
71. Abd Rahim N, Rafie SM. Sentiment analysis of social media data in vaccination. *Int J*. 2020;8. <https://doi.org/10.30534/ijeter/2020/60892020>
72. Yousefinaghani S, Dara R, Mubareka S, Papadopoulos A, Sharif S. An analysis of COVID-19 vaccine sentiments and opinions on Twitter. *Int J Infect Dis: IJID: Off Publ Int Soc Infect Dis*. 2021;108:256–62. <https://doi.org/10.1016/j.ijid.2021.05.059> PMID: 34052407
73. Hu T, Wang S, Luo W, Zhang M, Huang X, Yan Y, et al. Revealing public opinion towards COVID-19 vaccines with Twitter data in the United States: spatiotemporal perspective. *J Med Internet Res*. 2021;23(9):e30854. <https://doi.org/10.2196/30854> PMID: 34346888
74. Umair A, Masciari E. Sentimental and spatial analysis of covid-19 vaccines tweets. *J Intell Inf Syst*. 2023;60(1):1–21. <https://doi.org/10.1007/s10844-022-00699-4> PMID: 35462784
75. Evans W, Bingenheimer J, Long M, Ndiaye K, Donati D, Rao N, et al. Outcomes of a social media campaign to promote COVID-19 vaccination in Nigeria. *Plos One*. 2023;18(9):e0290757. <https://doi.org/10.1371/journal.pone.0290757>
76. Koku E, Johnson-Yengbeh N, Muhr A. Addressing COVID-19 vaccine hesitancy and uptake among African immigrants: lessons from a community-based outreach program. *J Racial Ethnic Health Disparit*. 2024. 1–15. <https://doi.org/10.1007/s40615-024-01947-9>
77. Harvey H, Reissland N, Mason J. Parental reminder, recall and educational interventions to improve early childhood immunisation uptake: a systematic review and meta-analysis. *Vaccine*. 2015;33(25):2862–80. <https://doi.org/10.1016/j.vaccine.2015.04.085> PMID: 25944299
78. Lemaitre T, Carrier N, Farrands A, Gosselin V, Petit G, Gagneur A. Impact of a vaccination promotion intervention using motivational interview techniques on long-term vaccine coverage: the PromoVac strategy. *Human Vaccines Immunotherap*. 2019;15(3):732–9. <https://doi.org/10.1080/21645515.2018.1549451> PMID: 30457421